Identification of a neuropeptide precursor protein that gives rise to a "cocktail" of peptides that bind Cu(II) and generate metal-linked dimers

Jones, CE; Zandawala, M; Semmens, DC; Anderson, S; Hanson, GR; Janies, DA; Elphick, MR

For additional information about this publication click this link.
http://qmro.qmul.ac.uk/xmlui/handle/123456789/11309

Identification of a neuropeptide precursor protein that gives rise to a "cocktail" of peptides that bind Cu(II) and generate metal-linked dimers

Christopher E. Jones[a⊥]*, Meet Zandawala[b⊥], Dean C. Semmens[b], Sarah Anderson[b],

Graeme R. Hanson[c‖], Daniel A. Janies[d] and Maurice R. Elphick[b]*

[a.]School of Science and Health, Western Sydney University, Locked bag 1797,

Penrith, 2751, New South Wales, Australia.

[b.]School of Biological & Chemical Sciences, Queen Mary University of London,

Mile End Road, London, E1 4NS, UK.

[c.] Centre for Advanced Imaging, The University of Queensland, Brisbane,

Queensland, 4072, Australia

[d.]Department of Bioinformatics and Genomics, University of North Carolina at Charlotte,

Charlotte, NC 28223 USA

*To whom correspondence should be addressed:

Christopher E. Jones, School of Science and Health, Western Sydney University, Locked bag 1797, Penrith, NSW, 2759, Australia. Tel: +61 29685 9908; Fax: +61 2 9685 9915; E-mail: c.jones@uws.edu.au

or

Maurice R. Elphick, School of Biological & Chemical Sciences, Queen Mary University of London, Mile End Road, London, E1 4NS, UK. Tel: 0207 882 6664; Fax: 0207 882 7732; E-mail: m.r.elphick@qmul.ac.uk

⊥ These authors contributed equally.

‖ Deceased, 16/07/1955 – 25/02/2015

Abstract

Background

Neuropeptides with an Amino Terminal Cu(II), Ni(II) Binding (ATCUN) motif (H_2N-xxH) bind Cu(II)/Ni(II) ions. Here we report the novel discovery of a neuropeptide precursor that gives rise to a "cocktail" of peptides that bind Cu(II)/Ni(II) and form ternary complexes – the L-type SALMFamide precursor in the starfish *Asterias rubens*.

Methods

Echinoderm transcriptome sequence data were analysed to identify transcripts encoding precursors of SALMFamide-type neuropeptides. The sequence of the L-type SALMFamide precursor in the starfish *Asterias rubens* was confirmed by cDNA sequencing and peptides derived from this precursor (e.g. AYHSALPF-NH_2, GYHSGLPF-NH_2 and LHSALPF-NH_2) were synthesised. The ability of these peptides to bind metals was investigated using UV/Vis, NMR, circular dichroism and EPR spectroscopy.

Results

AY$\underline{H}$SALPF-NH_2 and GY$\underline{H}$SGLPF-NH_2 bind Cu(II) and Ni(II) and generate metal-linked dimers to form ternary complexes with LHSALPF-NH_2. Investigation of the evolutionary history of the histidine residue that confers these properties revealed that it can be traced to the common ancestor of echinoderms, which is estimated to have lived ~500 million years ago. However, L-type precursors comprising multiple SALMFamides with the histidine residue forming an ATCUN motif appears to be a feature that has evolved uniquely in starfish (Asteroidea).

General Significance

The discovery of a SALMFamide-type neuropeptide precursor protein that gives rise to a "cocktail" of peptides that bind metal ions and generate metal-linked dimers provides a new insight on ATCUN motif-containing neuropeptides. This property of L-type SALMFamides

in the Asteroidea may be associated with a role in regulation of the unusual extra-oral feeding behavior of starfish.

1.0 Introduction

Neuropeptides are neuronal intercellular signalling molecules that act as neurotransmitters, neuromodulators or neurohormones and regulate many physiological processes and behaviours in humans and other animals [1]. They are derived from larger precursor proteins and are subject to post-translational modifications that are important for function; for example, in many neuropeptides a C-terminal glycine residue is converted to an amide group. Furthermore, in some neuropeptides the presence of a histidine residue can confer the ability to bind metal ions. In particular, the presence of an Amino Terminal Cu(II), Ni(II) Binding (ATCUN) motif, where a histidine residue is specifically located in the third position from the N-terminus (i.e. H_2N-xxH, where x is variable), has been found to confer high affinity binding of Cu(II) and Ni(II). The ATCUN motif was originally characterized in albumins but subsequently it has been demonstrated that other peptides/proteins with an ATCUN motif also bind Cu(II) and/or Ni(II) ions [2, 3]. In 1995 Harford and Sarkar demonstrated that the mammalian neuropeptide neuromedin C, which has the N-terminal sequence Gly-Asn-His, binds both Cu(II) and Ni(II) specifically. Furthermore, the authors speculated that this property of neuromedin C may have relevance to neurological deficits associated with copper metabolism disorders, such as Menkes disease and Wilson disease [4]. More recently, Russino et al. reported that the mammalian tachykinin-type peptide neurokinin B, which contains an ATCUN motif, binds Cu(II) ions in an unusual $[Cu^{II}(NKB)_2]$ complex [5]. Furthermore, although Cu(II) binding substantially alters the structure of neurokinin B, the ability of $[Cu^{II}(NKB)_2]$ to activate the NKB receptor was not impeded. It was speculated that NKB may have a role in protecting cells from the effects of neuronally released copper. Several other members of the tachykinin peptide family have also been shown to coordinate copper ions, yet the physiological consequences remain to be determined [6, 7].

Here we report the novel discovery of a neuropeptide precursor protein that gives rise to a "cocktail" of neuropeptides that bind Cu(II) – the starfish L-type SALMFamide precursor. SALMFamide neuropeptides occur in species belonging to the phylum Echinodermata, which includes starfish, brittle stars, sea urchins, sea cucumbers and feather stars [8]. The first members of this neuropeptide family to be identified, S1 and S2, were both isolated from the starfish species *Asterias rubens* and *Asterias forbesi*. S1 is an octapeptide with the amino acid sequence GFNSALMF-NH$_2$ and S2 is a dodecapeptide with the amino acid sequence SGPYSFNSGLTF-NH$_2$ [9, 10]. Subsequently, SALMFamides were identified in other echinoderms, including GFSKLYF-NH$_2$ and SGYSVLYF-NH$_2$ from the sea cucumber *Holothuria glaberrima* and GYSPFMF-NH$_2$ and FKSPFMF-NH$_2$ from the sea cucumber *Apostichopus japonicus* [11]. Identification of these holothurian neuropeptides revealed the existence of two types of SALMFamides. Firstly, L-type SALMFamides that have the C-terminal motif SxLxF-NH$_2$ (e.g. S1, S2, GFSKLYF-NH$_2$ and SGYSVLYF-NH$_2$) and secondly, F-type SALMFamides that have the C-terminal motif SxFxF-NH$_2$ (GYSPFMF-NH$_2$ and FKSPFMF-NH$_2$).

Investigation of the bioactivity of SALMFamides in echinoderms has revealed that both L-type and F-type SALMFamides act as muscle relaxants [12]. For example, S1 and S2 both cause dose-dependent relaxation of apical muscle, tube foot and cardiac stomach preparations from the starfish *A. rubens* [13, 14]. Furthermore, S2 exhibits higher potency/efficacy than S1, which provided a rationale for investigation of a structural basis for this difference in bioactivity. By testing chimeric analogs of S1 and S2, it was found that it is the C-terminal region of the peptides that is the primary determinant of their differing potency/efficacy [15, 16]. However, the N-terminal tetrapeptide (SGPY) of S2 contributes to its bioactivity and confers on S2 the property to self-associate and form highly structured multimers at high concentrations [15]. Interestingly, addition of the SGPY tetrapeptide to the

N-terminus of S1 confers structure that is not observed with the S1 peptide, but without enhancing bioactivity. Thus, the differing bioactivity of S1 and S2 is determined by a complex interplay of sequence and conformation.

Advances in genome/transcriptome sequencing have enabled determination of the sequences of SALMFamide neuropeptide precursor proteins. For example, sequencing of the genome and transcriptome of the starfish *Patiria miniata* revealed: 1) an "L-type" precursor comprising S1 and six other L-type SALMFamides and 2) an "F-type" precursor comprising eight F-type or F-type-like SALMFamides and an S2-like peptide (L-type). Furthermore, comparative analysis of sequence data from a variety of echinoderm species has enabled investigation of the evolution of SALMFamide precursors [17, 18]. The phylum Echinodermata comprises five extant classes, Asteroidea (starfish), Ophiuroidea (brittle stars), Echinoidea (sea urchins, sand dollars), Holothuroidea (sea cucumbers) and Crinoidea (feather stars and sea lilies), and the phylogenetic relationships of these classes have been determined. Thus, the Asteroidea and Ophiuroidea are sister classes (the Asterozoa) and the Echinoidea and Holothuroidea are sister classes (the Echinozoa), with the Crinoidea basal to the Asterozoa and Echinozoa [19-26]. This phylogeny has provided a framework to reconstruct the evolution of SALMFamide precursors in the phylum Echinodermata. In crinoid species only a single SALMFamide precursor has been identified, whereas asterozoan and echinozoan species have both an L-type and an F-type precursor. It has therefore been postulated that the L-type and F-type precursors found in asterozoans and echinozoans may have arisen by duplication of a common ancestral-type precursor similar to that found in extant crinoids [17].

Here we have obtained additional sequences of SALMFamide precursors in echinoderm species representing the five extant classes. Comparative analysis of the sequences of echinoderm SALMFamide precursors revealed that several neuropeptides

derived from L-type SALMFamide precursors in starfish have an ATCUN motif. For example AY<u>H</u>SALPF-NH$_2$, a neuropeptide that has been identified previously in the starfish species *Marthasterias glacialis* [27]. In addition, one of the peptides derived from L-type SALMFamide precursors in starfish (e.g. LHSALPF-NH$_2$) has a histidine in the same position as the tripeptide Gly-His-Lys (GHK), a well-studied naturally occurring human copper-binding growth factor [28]. We show here that L-type SALMFamides in the starfish *A. rubens* that have an ATCUN motif are able to bind Cu(II) and Ni(II). Furthermore, Cu(II) binding to these peptides facilitates formation of ternary complexes with LHSALPF-NH$_2$. The evolutionary and functional significance of these properties of neuropeptides derived from the L-type SALMFamide precursor in starfish is discussed.

2.0 Materials and Methods

2.1 Transcriptome sequencing

The sequences of SALMFamide precursors have been determined in species representing all five echinoderm classes, as reported previously [17, 18]. Here we have obtained additional transcriptome sequence data from other species belonging to each of the five echinoderm classes: the starfishes *Asterias rubens* and *Remaster gourdoni* (class Asteroidea), the brittle stars *Ophioderma brevispinum* and *Astrophyton muricatum* (class Ophiuroidea), the sea urchins *Arbacia punctulata* and *Eucidaris tribuloides* (class Echinoidea), the sea cucumbers *Psolus spp*, *Stichopus chloronatus* and *Pannychia moseleyi* (class Holothuroidea) and the feather stars *Isometra vivipara* and *Oligometra serripinna* (class Crinoidea).

Asterias rubens radial nerve cord transcriptome sequence data were obtained as reported previously [29]. For the other echinoderm species, RNA was extracted from tube feet (*Remaster gourdoni*), arms (*Ophioderma brevispinum*, *Astrophyton muricatum*), body wall (*Arbacia punctulata*, *Eucidaris tribuloides*, *Psolus spp*, *Stichopus chloronatus*, *Pannychia moseleyi*) or pinnules (*Isometra vivipara*, *Oligometra serripinna*) and then subjected to RNA-Seq sequencing on an Illumina Hiseq 2000 platform (100 base pairs, paired end). Reads for each of the samples were filtered by quality score (cutoff threshold > Q20) using fastxtrimmer and Illumina adapters were removed using fastxclipper, which are both components of the fastx toolkit (http://hannonlab.cshl.edu/fastx_toolkit/). *De novo* assembly of contigs was then performed using Trinity on a high memory computer cluster using 500 GB of RAM and 24 CPUs [30].

2.2 Cloning and sequencing of the L-type SALMFa precursor cDNA from *A. rubens*

SALMFamides derived from the *A. rubens* L-type SALMFamide precursor were selected for the metal-binding studies described below. To facilitate this it was first necessary to confirm, by cDNA cloning and sequencing, the sequence of the precursor predicted from Illumina transcriptome sequencing. Total RNA from radial nerve cords of *A. rubens* was isolated using the Total RNA Isolation System (Promega) and used for cDNA synthesis using the Quantitect Reverse Transcription Kit (QIAgen). The full-length cDNA of the *A. rubens* L-type SALMFa precursor, including 5′ and 3′ untranslated regions (UTR), was amplified by PCR using Phusion high-fidelity PCR master mix (NEB) and the oligos 5′-TAGCTACTTGACACA-3′ and 5′-ATATGACTAGTTGAGAGAGG-3′, which were designed using Primer3 software (http://bioinfo.ut.ee/primer3-0.4.0/). The PCR product was gel-extracted and purified using a QIAquick gel extraction kit (QIAgen) before being blunt-end cloned into a pBluescript SKII (+) vector (Agilent Technologies) cut with a *Eco*RV-HF restriction endonuclease (NEB). The clone was then sequenced (Eurofins Genomics) from the T7 and pCR3.1-BGH-rev sequencing primer sites.

2.3 Neuropeptide synthesis and metal titrations

The *A. rubens* L-type SALMFamides AYHSALPF-NH$_2$, GYHSGLPF-NH$_2$ and LHSALPF-NH$_2$ were synthesised by Synpeptide (Shanghai, China) and were >95% pure as determined by mass spectrometry and NMR. The lyophilized peptides were weighed and dissolved in the required buffer (10 mM nEM unless otherwise stated) on the day of use. The peptide concentration was estimated using the extinction coefficient of the single tyrosine amino acid (ε_{280nm} = 1280 M^{-1}cm^{-1}) or from the measured mass taking into consideration the presence of ~30% water. Stock (0.5 M) solutions of copper and nickel were prepared as CuCl$_2$·2H$_2$O and NiCl$_2$·2H$_2$O in water and diluted to working solutions on the day of use.

Metal addition during titrations was achieved using a 10 μL Hamilton gastight syringe. The spectrum of metal-free peptide was subtracted from the spectrum after each metal addition and dilution effects were taken into account during processing of the spectra.

2.4 Electronic Spectroscopy

UV/Visible electronic spectra (300 nm – 700 nm) were acquired on a Perkin-Elmer U-3100 using a 10 mm pathlength cuvette.

2.5 Circular dichroism (CD) Spectroscopy

CD spectra were collected on a Jasco J810 spectrometer. Spectra were routinely collected over the range 300 nm to 700 nm using a 10 mm cuvette with sampling every 1 nm. A minimum of 10 spectra were obtained and averaged, prior to smoothing using an 11-point moving average method in the Jasco software.

2.6 Electron Paramagnetic Resonance (EPR) Spectroscopy

Continuous wave EPR spectra at ~9.4 GHz (X-band) were obtained on a Bruker Elexsys E500 spectrometer operated with Bruker Xepr software and equipped with a super high-Q cavity. Calibration of the field was achieved using an ER036TM teslameter and the microwave frequency was calibrated with an EIP548B frequency counter. Stable temperatures of $150 \pm 5K$ were achieved using a nitrogen gas flow through system linked to a Eurotherm B-VT-2000 variable temperature controller. Instrument settings were: modulation frequency 100 kHz; modulation amplitude 0.63G; microwave power 10 – 20 mW; number of scans 40 – 60; time constant 5.12 ms; sweep time 84 s. Spectra were baseline corrected using a polynomial function and high frequency noise was removed using Fourier filtering available in the Xepr software. Spectra were simulated using the least-squares fitting

algorithm in Easyspin running in Matlab R2014a [31]. The copper hyperfine and Zeeman

interactions were initially simulated using matrix diagonalization, and perturbation theory

was used after inclusion of nitrogen nuclei to simulate the nitrogen superhyperfine

interactions. Where the presence of multiple absorbing species was apparent (i.e.

[Cu^{II}LHSALPF-NH_2]) the magnetic parameters were estimated directly from the spectrum.

Linewidths were fit using a correlated distribution of g- and A-values [32].

2.7 Nuclear Magnetic Resonance (NMR) Spectroscopy

NMR spectra were acquired on a Bruker Avance 500 MHz spectrometer equipped with a 5

mm TXI BBI probe and controlled using TopSpin 2.1 (Bruker Biospin, Germany). Samples

were prepared in 90% H_2O/10% D_2O and the pH was adjusted using aliquots of concentrated

HCl or NaOH. Proton spectra were acquired over a 10 ppm spectral width comprising 64K

complex points, and the residual water signal was supressed using a W5 watergate sequence.

Spectra were processed using a $\pi/2$ shifted sine squared window function in SpinWorks 4

[33].

3.0 Results

3.1 Identification of novel SALMFamide precursor sequences

Sequences encoding SALMFamide precursors have been identified previously in species representing each of the five classes in Echinodermata [17, 18]. These include sequences from *Patiria miniata* (Class Asteroidea; Order Valvatida), *Luidia senegalensis* (Class Asteroidea; Order Paxillosida), *Ophionotus victoriae* (Class Ophiuroidea; Order Ophiurida), *Ophiothrix angulata* (Class Ophiuroidea; Order Ophiurida), *Strongylocentrotus purpuratus* (Class Echinoidea; Order Echinoida), *Lytechinus variegatus* (Class Echinoidea; Order Temnopleuroida), *Apostichopus japonicus* (Class Holothuroidea; Order Aspidochirotida), *Leptosynapta tenuis* (Class Holothuroidea; Order Apodida) and *Antedon mediterranea* (Class Crinoidea; Order Comatulida) and *Aporometra wilsoni* (Class Crinoidea; Order Comatulida).

Here, by analysis of new transcriptome sequence data, we have identified SALMFamide precursors in other echinoderm species, which include *Asterias rubens* (Class Asteroidea, Order Forcipulatida), *Remaster gourdoni* (Class Asteroidea, Order Velatida), *Ophioderma brevispinum* (Class Ophiuroidea, Order Ophiurida), *Astrophyton muricatum* (Class Ophiuroidea, Order Euryalida), *Arbacia punctulata* (Class Echinoidea, Order Arbacioida), *Eucidaris tribuloides* (Class Echinoidea, Order Cidaroida), *Psolus spp* (Class Holothuroidea; Order Dendrochirotida), *Stichopus chloronatus* (Class Holothuroidea; Order Aspidochirotida), *Pannychia moseleyi* (Class Holothuroidea, Order Elasipodida), *Isometra vivipara* (Class Crinoidea, Order Comatulida) and *Oligometra serripinna* (Class Crinoidea, Order Comatulida).

3.2 Comparative analysis of echinoderm SALMFamide neuropeptide sequences: identification of conserved histidine residues

12

Determination of the sequences of SALMFamide precursors in species from each of the five echinoderm classes enabled comparison of the sequences of the constituent neuropeptides and identification of conserved characteristics. Thus, Figure 1 shows C-terminally aligned neuropeptides derived from L-type SALMFamide precursors in asterozoan and echinozoan species, with data from three species in each class shown. The presence of a leucine or an isoleucine residue (highlighted in red) in the third position from the C-terminal amide is characteristic feature of the majority of the neuropeptides, as expected for L-type SALMFamide precursor derived peptides. Furthermore, another conserved feature is the presence of a histidine residue (highlighted in turquoise) in the sixth position from the C-terminal amide, with at least one of the peptides in all but one of the twelve species having this feature. However, it is most strikingly apparent in starfish species, where six out of seven or five out of six of the SALMFamides have this characteristic. With respect to the N-terminus, the position of the conserved histidine residue is variable, ranging from position two to position eight. However, in starfish four of the five or six peptides with a histidine residue have the histidine in the third position from N-terminus. This is noteworthy because, as highlighted in the introduction, the presence of a histidine residue in this position is known to confer on peptides and proteins the ability to bind copper and nickel ions with high affinity. Hence, the H_2N-xxH motif is known as an Amino Terminal Cu(II), Ni(II) Binding (ATCUN) motif.

<<**INSERT FIGURE 1**>>

Having identified the occurrence of conserved histidine residues in SALMFamides derived from L-type precursors, we investigated if this is also a conserved feature of SALMFamides derived from F-type precursors. Thus, Figure 2 shows C-terminally aligned

neuropeptides derived from F-type SALMFamide precursors in asterozoan and echinozoan species, with data from three species in each class shown. The presence of a phenylalanine residue or a structurally similar tyrosine residue (highlighted in yellow) in the third position from the C-terminal amide is a characteristic feature of the majority of the neuropeptides, as expected for F-type SALMFamide precursor derived peptides. However, unlike in L-type SALMFamide precursor derived peptides, histidine residues are not prevalent in F-type SALMFamide precursor derived peptides (Fig. 2) and only one peptide (in the sea urchin *Arbacia punctulata*) has a histidine residue in the sixth position from the C-terminal amide.

<<INSERT FIGURE 2>>

Lastly, we analysed the sequences of neuropeptides derived from the singular SALMFamide precursors that have been identified in crinoids. This revealed an interesting pattern in the occurrence of histidine residues, with conserved histidines present in L-type peptides located at the extremities of the precursors. Thus, in all three crinoid species analysed here, the first and last neuropeptide in the precursor proteins is an L-type SALMFamide with a histidine residue located at the sixth position from the C-terminal amide, a feature that they share with the majority of SALMFamides derived from L-type SALMFamide precursors in asterozoan and echinozoan species (Fig. 3). By way of contrast, the twelve neuropeptides that form the core of the crinoid SALMFamide precursors mostly have phenylalanine, tyrosine or leucine residues at position three with respect to the C-terminal amide and typically do not have histidine residues. The occurrence at the extremities of crinoid SALMFamide precursors of L-type SALMFamides that have a histidine residue at position six with respect to C-terminal amide is interesting because it suggests that peptides with these characteristics may have given rise to the structurally related peptides that are

14

found in asterozoan and echinozoan L-type SALMFamide precursors. Accordingly, our data indicate that the evolutionary origin of L-type SALMFamides with a conserved histidine residue at position six with respect to the C-terminal amide can be traced back to the common ancestor of extant echinoderms. However, it is in the Asteroidea that peptides with this characteristic are most prevalent and furthermore the histidine typically occupies the third position from the N-terminus, forming a potential Cu(II) and Ni(II) binding site. This feature of SALMFamides derived from the L-type SALMFamide precursor in starfish is interesting from an evolutionary and functional perspective and therefore, as described below, we have investigated if these peptides do indeed bind Cu(II) and Ni(II) ions. To do this we synthesized and analysed neuropeptides derived from the L-type SALMFamide precursor in the common European starfish *A. rubens*.

<<**INSERT FIGURE 3**>>

3.3 Determination of the sequence of a cDNA encoding the L-type SALMFamide precursor in *A. rubens*

Cloning and sequencing of a 1028 bp cDNA encoding the *A. rubens* L-type SALMFamide precursor confirmed the predicted amino acid sequence obtained from transcriptome sequence data. Thus, the *A. rubens* L-type SALMFamide precursor is a 210 residue protein with a predicted 23-residue signal peptide and seven L-type SALMFamides that are bounded by dibasic cleavage sites (Fig. S1). Four of these peptides (AYHSALPF-NH_2, AYHTGLPF-NH_2, GYHSALPF-NH_2 and GYHSGLPF-NH_2) contain the ATCUN motif H_2N-xxH (Fig. 1 and S1). Two other peptides (PAGASAFHSALSY-NH_2 and LHSALPF-NH_2) contain a histidine residue but it is not in the third position from the N-terminus, whilst the peptide S1 (GFNSALMF-NH_2) lacks a histidine residue altogether.

15

3.4 Electronic and circular dichroism spectroscopy highlights coordination of copper and nickel to L-type SALMFamides

To investigate the copper binding ability of peptides derived from the *A. rubens* L-type SALMFamide precursor, we chose three representative peptides potentially containing copper sites: AYHSALPF-NH$_2$, GYHSGLPF-NH$_2$ and LHSALPF-NH$_2$. We initially used electronic spectroscopy to probe metal binding. Figure 4A shows the spectra obtained after titration of Cu^{2+} or Ni^{2+} into AYHSALPF-NH$_2$. Addition of Cu^{2+} to AYHSALPF-NH$_2$ gives rise to an absorption band centred on 520 nm and the intensity tends to stop increasing with copper addition at around one equivalent (Fig. 4B). An absorption maximum of 520 nm is indicative of Cu^{2+} bound with only nitrogen coordination [2]. Titration of Ni^{2+} generates an absorption band at 420 nm (Fig. 4A) and, in contrast to Cu^{2+}, the slope of the binding curve changes, rather than plateauing, at one equivalent (Fig. 4B). A peak at 420 nm is suggestive of Ni^{2+} bound in a square-planar, four-coordinate geometry [34]. Both the stoichiometry and wavelength maxima of Cu^{2+} and Ni^{2+} binding are entirely consistent with coordination of these metals to an ATCUN site. As expected, titration of these metals into GYHSGLPF-NH$_2$ produced identical results (Fig. 4C, D). The ATCUN motif generally binds copper and nickel via the N-terminal nitrogen, the histidine imidazole nitrogen, and intervening amide nitrogens (i.e. $\{N_a, 2N^-, N_{Im}\}$) and therefore the nature of the amino acid side chains is of less importance, especially in this case where only the presence of a glycine or alanine differentiates the motif in AYHSALPF-NH$_2$ and GYHSGLPF-NH$_2$. A feature of an ATCUN site is the lack of changes to the absorption maximum as a function of pH [2]. Accordingly, the maximum wavelength of [Cu^{II}GYHSGLPF-NH$_2$] (520 nm) remains constant from ~ pH 5 (Fig. S2A). In contrast to AYHSALPF-NH$_2$ and GYHSGLPF-NH$_2$, titration of Cu^{2+} into LHSALPF-NH$_2$ generates a peak at 600 nm, but, similar to the previous peptides, the absorbance plateaus at around one equivalent Cu^{2+} (Fig. 4E, F). An absorbance at 600 nm

suggests this peptide contains one or more oxygen ligands in its coordination sphere. A pH titration of this peptide shows the 600 nm wavelength maximum remains constant until higher pH values (> pH 9) where increasing absorption at wavelengths <600 nm suggests incorporation of an additional nitrogen donor (Fig. S2B) [28].

<<INSERT FIGURE 4>>

To further examine the copper binding sites we used NMR. The presence of low concentrations of paramagnetic Cu^{2+} tends to broaden peaks associated with protons lying within ~7Å of the metal. Addition of ~0.1 equivalent Cu^{2+} to GYHSGLPF-NH_2 results in selective broadening of the C_2H (7.68 ppm) and C_4H (6.92 ppm) protons of the imidazole ring (Fig. 5A) which tends to confirm His3 is a nitrogen donor. Some broadening of peaks due to the His3 Hβ protons (~3.61 ppm, shifted downfield due to ring current effects of Tyr2) is also observed (see Fig. S3 for expanded regions). Coordination of copper to the His3 amide and imidazole nitrogen ($N\delta_1$) could account for the perturbation of the beta protons. Additionally, peaks due to Tyr2 Hβ protons also show some broadening consistent with coordination to the nearby amide of Tyr2 (Fig. 5A, Fig. S3). In a similar manner addition of Cu^{2+} to LHSALPF-NH_2 results in a loss of peaks due to histidine imidazole protons (Fig. 5B). It is difficult to assess changes to the His3 Hβ peaks (~ 3.15 ppm, Fig. 5B) given overlap with Phe8 Hβ. A change in both the broadness and chemical shift is readily observed for the Leu1 Hβ peaks (~1.6 ppm), and to some extent the Hδ peaks (~0.9 ppm) (Fig. S3B), which suggests coordination to the nearby amide nitrogen of the amino acid. Intriguingly, despite having the same ratio of copper to peptide in both GYHSGLPF-NH_2 and LHSALPF-NH_2 the His imidazole peaks in the [Cu^{II}LHSALPF-NH_2] sample have completely broadened and disappeared, but remain to some extent in the [Cu^{II}GYHSGLPF-NH_2] sample (Fig. 5). This

17

suggests that the different copper-binding sites in these peptides have different copper on/off rates (on the NMR timescale) with [Cu^{II}LHSALPF-NH$_2$] at a comparatively faster rate than [Cu^{II}GYHSGLPF-NH$_2$]. The C$_2$H and C$_4$H peaks observed in the slowly exchanging [Cu^{II}GYHSGLPF-NH$_2$] spectrum (Fig. 5A) presumably arise from the apo form of the complex.

<<INSERT FIGURE 5>>

We next analysed the copper-complexes by circular dichroism (CD) spectroscopy. CD spectroscopy is a useful tool to analyse Cu^{2+} complexes because the d-d transitions that overlap to give a single broad peak in electronic spectroscopy can often be resolved into positive and negative peaks in CD [35]. The CD spectrum of [Cu^{II}GYHSGLPF-NH$_2$] is shown in Figure 6A (the spectrum of [Cu^{II}AYHSALPF-NH$_2$] has identical bands and is not shown). Positive bands are apparent at 316 nm and 490 nm and a weaker negative band appears at 570 nm. The bands at 490 nm and 570 nm can be attributed to d-d transitions, whereas a band around 320 nm may be attributed to an amide nitrogen → Cu^{2+} charge transfer (CT). In line with the absorption spectroscopy, the intensity of the bands tends to stop increasing at one equivalent Cu^{2+} (Fig. 6B). The visible CD spectrum of [Cu^{II}GYHSGLPF-NH$_2$] is strikingly similar to the copper-bound peptides GGH and DAHK, as well as that of copper-bound full length human serum albumin, suggesting similar coordination in all [35, 36]. The ATCUN motif is known to have high affinity for copper (K$_d$ ~ 10^{-12} – 10^{-14} M) and should out-compete the weaker copper chelator glycine [37]. Titration of [Cu^{II}GYHSGLPF-NH$_2$] with glycine (up to 7× molar excess vs. copper) caused no apparent change to the CD spectrum of [Cu^{II}GYHSGLPF-NH$_2$] which tends to support binding via a high affinity ATCUN motif (data not shown). Further analysis of the copper

18

affinity of the SALMFamide peptides was not undertaken. The CD spectra obtained during a Cu^{2+} titration of LHSALPF-NH$_2$ are shown in Figure 6C. The spectra have a negative peak at 300 nm, a positive peak at 346 nm and a broad positive feature around 600 nm, and all are relatively low intensity and largely identical to the CD spectrum of [Cu^{II}GHK] [36]. The peak at 300 nm may be attributed to an amide nitrogen $\rightarrow Cu^{2+}$ CT, whereas the 346 nm peak is likely due to an imidazole nitrogen $\rightarrow Cu^{2+}$ CT, which is further supported by an absence of this peak in copper-bound tripeptides that lack a histidine [28, 35].

<<**INSERT FIGURE 6**>>

3.5 EPR spectroscopy predicts presence of a copper-linked ternary complex between GYHSGLPF-NH$_2$ and LHSALPF-NH$_2$.

The X-band (~9 GHz) EPR spectra of [Cu^{II}GYHSGLPF-NH$_2$] and [Cu^{II}LHSALPF-NH$_2$], each with a Cu^{2+}:peptide ratio of 0.96, are shown in Figure 7A and 7B respectively (the spectrum of [Cu^{II}AYHSALPF-NH$_2$] is identical to that of [Cu^{II}GYHSGLPF-NH$_2$] and is not shown) . The EPR spectra for both reveal an axially symmetric Cu(II) centre (i.e. $g_x = g_y \neq g_z$). For [Cu^{II}GYHSGLPF-NH$_2$] nitrogen superhyperfine (shf) coupling is apparent in the g_x, g_y (perpendicular, $g\perp$) region between 315 – 350 mT and analysis of the characteristic parallel g_z and $A_z(^{63}Cu)$ values suggests that the copper ion is in a 4-nitrogen environment (Table 1) at this pH (7.2) [38]. In [Cu^{II}LHSALPF-NH$_2$], the peak at $g\perp$ is considerably broadened, suggesting the presence of multiple species, however some nitrogen coupling is apparent. The presence of multiple species is supported by Cu(II) speciation studies with GHK where the presence of mono- and bis-complexes was indicated at pH values similar to those used here [3]. The parallel values (Table 1) of [Cu^{II}LHSALPF-NH$_2$] are different to those of [Cu^{II}(GYHSGLPF-NH$_2$)] and suggest inclusion of oxygen donors which has

19

increased g_z and decreased A_z relative to that observed for [Cu^{II}GYHSGLPF-NH$_2$]. Most likely the predominant [Cu^{II}LHSALPF-NH$_2$] species contains a CuN$_2$O$_2$ site which previous work suggests has average values of g_z = 2.238 – 2.265 and A_z = 0.0182 – 0.0187 cm^{-1} and is consistent with the electronic spectrum (Fig. 1E) [39]. When apo-GYHSGLPF-NH$_2$ is added to [Cu^{II}LHSALPF-NH$_2$] such that the peptides are equimolar (i.e. [Cu]:[total peptide] is ~0.5:1) then the spectrum in figure 7C is obtained. In this case the spectrum was best fit with Cu^{II} in a rhombically distorted environment (i.e. $g_x \neq g_y \neq g_z$). The g_z and A_z values are different to those of the pure copper-peptides and suggest that an additional nitrogen atom/s has been added to the coordination sphere [38]. Nitrogen coupling is not observed on the parallel components of the spectrum, however, compared to [Cu^{II}LHSALPF-NH$_2$] the linewidth in the perpendicular region has narrowed and the nitrogen shf coupling is more apparent. To improve resolution at $g_{x,y}$ the spectrum was differentiated and the expanded region (Fig. 7c) reveals the ^{14}N shf coupling in more detail. Theoretically, each copper hyperfine coupling is split into (2nI + 1) (I =1) lines, where n is the number of magnetically equivalent nitrogen ligands. Although it is instructive to examine the features at $g\perp$, in reality the number of lines is complicated by various factors such as the presence of multiple species, non-equivalent nitrogens and overlap with parallel features [40]. The experimental [Cu^{II}LHSALPF-NH$_2$] + apo-GYHSGLPF-NH$_2$ spectrum (Fig. 7c, exp) was fit assuming four and three nitrogens and the results (Fig. 7c 4N, 3N) suggest that the most likely coordination involves four nitrogen ligands. In neither case are the lines on the low field (320 – 325 mT) side of $g\perp$ well simulated, however on the high field side (335 – 338 mT) the four nitrogen simulation clearly fits the experimental spectrum more closely in both the line position and intensity than the three nitrogen simulation. The high field transitions are known to be particularly sensitive to the number of nitrogen ligands [40]. Thus, we predict that the predominant species formed when apo-GYHSGLPF-NH$_2$ is added to [Cu^{II}LHSALPF-NH$_2$]

has Cu^{II} in a four-nitrogen environment. The EPR spectrum does not resemble $[Cu^{II}GYHSGLPF-NH_2]$ indicating that apo-GYHSGLPF-NH$_2$ has not just abstracted all the copper from $[Cu^{II}LHSALPF-NH_2]$. It is likely that the oxygen donors observed in $[Cu^{II}LHSALPF-NH_2]$ have been replaced by nitrogens from apo-GYHSGLPF-NH$_2$ to form a copper-linked ternary complex. We predict that the histidine imidazole from GYHSGLPF-NH$_2$ is a nitrogen contributor the ternary complex. This result is not unprecedented, as a previous study showed addition of the amino acid histidine to a solution of $[Cu^{II}GHK]$ generated a 4N complex where the oxygen donor in $[Cu^{II}GHK]$ was displaced by a nitrogen from the histidine imidazole group [36]. Collection of spectra at alternative frequencies, such as S-band (~ 4 GHz) which avoids broadening due to g- and A-strain correlations, may allow nitrogen coupling to be more completely analysed.

We next wondered that if $[Cu^{II}LHSALPF-NH_2]$ can form 4N complexes with apo-GYHSGLPF-NH$_2$, then why does copper titration of LHSALPF-NH$_2$ by UV/Vis spectroscopy (Fig. 4E, F) show a simple 1:1 stoichiometry with a peak at 600 nm indicative of N/O coordination, when the 4N mononuclear binary complex $[Cu^{II}(LHSALPF-NH_2)_2]$ can presumably be formed? Given that NMR shows different copper on/off rates for the complexes then maybe the timescale of the UV/Vis experiment accounts for the observed result. To explore this $[Cu^{II}LHSALPF-NH_2]$ (Fig. 7D) was scanned, left at room temperature for 2 hours then re-scanned. The resultant spectrum (Fig. 7D) shows that the d-d transitions are now much broader than in the initial sample and there is increased absorption at wavelengths shorter than 600 nm (no evidence of aggregation was observed). Taken together with the EPR data, this suggests that initially a simple $[Cu^{II}LHSALPF-NH_2]$ complex with a 2N2O donor set is formed, but over time other species such as a 4N $[Cu^{II}(LHSALPF-NH_2)_2]$ having absorption around 500 nm also occur. Along with ternary complexes, these species

may also contribute to the EPR spectrum (Fig. 7c) which increases the difficulty of accurately simulating the nitrogen coupling.

<<INSERT FIGURE 7>>

4.0 Discussion

In this study we analysed SALMFamide neuropeptide precursor sequences from species belong to the five extant classes of the phylum Echinodermata and established that peptides derived from the L-type SALMFamide precursor in starfish (class Asteroidea) were over represented with the N-terminal sequence H_2N-xxH. This sequence is a well-known copper-binding site termed an ATCUN-motif and suggested that these peptides should bind the metal. Using a range of spectroscopic techniques we show that the L-type SALMFamides in the starfish species *A. rubens* that contain the motif (e.g. GY<u>H</u>SGLPF-NH$_2$) do indeed bind Cu(II) as well as Ni(II) ions. Taken together, the spectroscopic evidence indicates Cu(II) binding to these peptides involves the His3 imidazole nitrogen, the N-terminal nitrogen and intervening amide nitrogen atoms. Ni(II) binds in a similar manner resulting in a square-planar diamagnetic complex. In addition, we show that LHSALPF-NH$_2$, a heptapeptide derived from the *A. rubens* L-type SALMFamide precursor, can also bind copper but instead of four nitrogen atoms as ligands the complex initially includes oxygen atoms. Displacement of the oxygen ligand/s in the presence of GYHSGLPF-NH$_2$ resulted in the formation of a copper-linked ternary complex (a heterodimer). To the best of our knowledge, this is the first study to report the identification of a neuropeptide precursor that contains multiple Cu(II)-binding neuropeptides.

Comparative analysis of the sequences of SALMFamide precursors in echinoderms has provided a basis for investigation of the evolutionary history of the histidine residue that

confers on starfish L-type precursor-derived SALMFamides the ability to bind Cu(II) ions.

Crinoids, which occupy a basal position in echinoderm phylogeny, appear to have only a

single SALMFamide precursor, unlike asterozoans (starfish, brittlestars) and echinozoans

(sea urchins, sea cucumbers), which have an L-type and F-type SALMFamide precursor (Fig.

8). The crinoid SALMFamide precursor contains a core of twelve peptides that include F-

type-like SALMFamides. However, at both the N- and C-terminal extremities of the

precursor there are single L-type SALMFamides that have a histidine residue in the sixth

position from the C-terminus, in common with the majority of SALMFamides derived from

L-type precursors in asterozoans and echinozoans. We postulate, therefore, that following

duplication of a SALMFamide precursor gene in a common ancestor of the Asterozoa and

Echinozoa, one copy retained the L-type peptides with a histidine residue at position six with

respect to the C-terminal amide, lost other peptides and then gave rise to the L-type

SALMFamide precursors that occur in extant asterozoans and echinozoans. Conversely, the

other copy retained the core peptides that do not have conserved histidine residues, lost the L-

type peptides with a histidine residue at position six with respect to the C-terminal amide and

then gave rise to the F-type SALMFamide precursors that occur in extant asterozoans and

echinozoans. In surveying the occurrence in echinoderms of L-type SALMFamides with a

histidine residue at position six with respect to the C-terminal amide, it is striking that in

starfish (Asteroidea) these peptides are most abundant and have acquired the ATCUN motif

by virtue of the histidine occupying the third position from the N-terminus (Fig. 8).

<<INSERT FIGURE 8>>

The concentration of free copper ions in seawater is estimated in the range of 10^{-11} –

10^{-13} M, whilst the total dissolved copper concentration, which includes organically

complexed copper, is ~ 10^{-8} M [41-43]. It is likely that the copper content of the extracellular milieu in starfish is similar to that of seawater because these animals, like other marine invertebrates, are osmoconformers. Therefore, upon release from neurons L-type SALMFamides are likely to encounter copper ions at concentrations near the K_d established for ACTUN motif-containing peptides (10^{-12} – 10^{-14} M [37]) and therefore will compete for copper ions, even when taking into consideration the ligands present in seawater which can have high binding constants [42]. Interestingly, the SALMFamides, like other amidated neuropeptides, traffic through the Golgi network where they are C-terminally amidated by the copper-metalloenzyme peptidyl-glycine alpha-amidating monooxygenase [44]. The *trans*-Golgi contains copper because several proteins are loaded with copper in this cellular compartment during their biosynthesis. Although copper is pumped into the *trans*-Golgi as Cu^+ by the Menkes ATPase [45], it is not clear whether it stays as Cu^+ or if there is some oxidation to Cu^{2+}. It is therefore interesting to speculate that, rather than being metallated after release, L-type SALMFamides containing an ATCUN motif may in fact have copper already bound to them prior to release from starfish neurons.

At the molecular level, how may the presence of bound Cu(II) ions affect the bioactivity of L-type SALMFamides? Our previous studies on the prototypical SALMFamides S1 and S2, L-type SALMFamides that do not bind metal, indicate that their bioactivity is primarily determined by the C-terminal region of the peptides. The N-terminal tetrapeptide of S2 (SGPY) does, however, influence peptide structure by causing S2 to self-associate at high concentrations and form highly-structured multimers [15]. We predicted that S2's structure and activity may change as it diffuses away from sites of release and becomes less concentrated. Further, addition of the SGPY tetrapeptide to the N-terminus of S1 confers structure on this chimeric peptide that is not observed with the S1 peptide. Now we show that the L-type SALMFamide precursor-derived peptide LHSALPF-NH_2 can form a copper-

linked ternary complex (a heterodimer) with GYHSGLPF-NH$_2$, and the chemistry suggests that LHSALPF-NH$_2$ will form similar ternary complexes with any of the ATCUN-containing L-type SALMFamides. The formation of these copper complexes (monomers and dimers) may modify receptor binding or make the peptides more resistant to proteolysis. Interestingly, evidence that copper binding affects enzymatic degradation of neuropeptides has been reported recently. Herman et al. [46] reported that human gonadotropin-releasing hormone (GnRH), which has a histidine residue at position two, binds Cu^{2+} ions and this confers on GnRH increased resistance to enzymatic degradation in extracts of hypothalamic and pituitary tissue. Accordingly, the copper-linked ternary complexes of LHSALPF-NH$_2$ and ACTUN motif-containing L-type SALMFamides may likewise be more resistant to enzymatic degradation than the monomeric peptides in the absence of copper.

At the physiological level, previous studies have revealed that SALMFamide neuropeptides S1 and S2 cause dose-dependent relaxation of the starfish cardiac stomach *in vitro* and trigger cardiac stomach eversion *in vivo* (Melarange et al., 1999). This pharmacological effect of SALMFamides is of interest because starfish feed by everting their cardiac stomach over prey and partially digesting prey tissue externally. Therefore, it is proposed that SALMFamides may mediate neural control of cardiac stomach eversion during starfish feeding behaviour [12]. Furthermore, extraoral feeding is unique to starfish (Class Asteroidea) amongst extant echinoderms [47]. We speculate, therefore, that the acquisition and proliferation of L-type SALMFamides that have an ATCUN motif and bind copper ions in starfish may be associated with a role in regulating stomach eversion. For example, the secretion of proteases by cells in the mucosal epithelium of the cardiac stomach during feeding creates a proteolytic environment [47], which may have favoured acquisition of structural characteristics that protect SALMFamides from aminopeptidases. Therefore, in this

context, our findings may provide a basis for experimental studies in which the physiological

significance of copper-binding neuropeptides could be further investigated.

Acknowledgements

References

1.	Taghert, P.H. and M.N. Nitabach, **Peptide neuromodulation in invertebrate model systems**. Neuron, 76 (2012): pp. 82-97.DOI: 10.1016/j.neuron.2012.08.035.
2.	Harford, C. and B. Sarkar, **Amino terminal Cu(II)- and Ni(II)-binding (ATCUN) motif of proteins and peptides: metal binding, dna cleavage, and other properties.** Acc. Chem. Res., 30 (1997): pp. 123-130.DOI: 10.1021/ar9501535.
3.	Conato, C., H. Kozlowski, P. Mlynarz, F. Pulidori, and M. Remelli, **Copper and nickel complex-formation equilibria with Lys-Gly-His-Lys, a fragment of the matricellular protein SPARC**. Polyhedron, 21 (2002): pp. 1469-1474.DOI: Pii S0277-5387(02)00952-X.
4.	Harford, C. and B. Sarkar, **Neuromedin C binds Cu(II) and Ni(II) via the ATCUN motif: implications for the CNS and cancer growth**. Biochem. Biophys. Res. Commun., 209 (1995): pp. 877-82.DOI: 10.1006/bbrc.1995.1580.
5.	Russino, D., E. McDonald, L. Hejazi, G.R. Hanson, and C.E. Jones, **The tachykinin peptide neurokinin B binds copper forming an unusual [CuII(NKB)2] complex and inhibits copper uptake into 1321N1 astrocytoma cells**. ACS Chem. Neurosci., 4 (2013): pp. 1371-81.DOI: 10.1021/cn4000988.
6.	Kowalik-Jankowska, T., E. Jankowska, Z. Szewczuk, and F. Kasprzykowski, **Coordination abilities of neurokinin A and its derivative and products of metal-catalyzed oxidation**. J. Inorg. Biochem., 104 (2010): pp. 831-42.DOI: 10.1016/j.jinorgbio.2010.03.016.
7.	Pietruszka, M., E. Jankowska, T. Kowalik-Jankowska, Z. Szewczuk, and M. Smuzynska, **Complexation abilities of neuropeptide gamma toward copper(II) ions and products of metal-catalyzed oxidation**. Inorg. Chem., 50 (2011): pp. 7489-99. DOI: 10.1021/ic2002942.
8.	Elphick, M.R., **SALMFamide salmagundi: The biology of a neuropeptide family in echinoderms**. Gen. Comp. Endocrinol., 205 (2014): pp. 23-35. DOI 10.1016/j.ygcen.2014.02.012.
9.	Elphick, M.R., D.A. Price, T.D. Lee, and M.C. Thorndyke, **The SALMFamides: a new family of neuropeptides isolated from an echinoderm**. Proc. Bio.l Sci., 243 (1991): pp. 121-7.DOI: 10.1098/rspb.1991.0020.
10.	Elphick, M.R., J.R. Reeve, Jr., R.D. Burke, and M.C. Thorndyke, **Isolation of the neuropeptide SALMFamide-1 from starfish using a new antiserum**. Peptides, 12 (1991): pp. 455-9.DOI: 10.1016/0196-9781(91)90083-2.
11.	Ohtani, M., E. Iwakoshi, Y. Muneoka, H. Minakata, and K. Nomoto, **Isolation and characterization of bioactive peptides from the sea cucumber, Stichopus japonicus**. Peptide Science - Present and Future, (1999): pp. 419-420.DOI: 10.1007/0-306-46864-6_137.
12.	Elphick, M.R. and R. Melarange, **Neural control of muscle relaxation in echinoderms**. J. Exp. Biol., 204 (2001): pp. 875-85.
13.	Melarange, R., D.J. Potton, M.C. Thorndyke, and M.R. Elphick, **SALMFamide neuropeptides cause relaxation and eversion of the cardiac stomach in starfish.** Proc. Biol. Sci., 266 (1999): pp. 1785-1789.DOI: 10.1098/rspb.1999.0847.
14.	Melarange, R. and M.R. Elphick, **Comparative analysis of nitric oxide and SALMFamide neuropeptides as general muscle relaxants in starfish**. J. Exp. Biol., 206 (2003): pp. 893-9. DOI: 10.1242/jeb.00197.
15.	Otara, C.B., C.E. Jones, N.D. Younan, J.H. Viles, and M.R. Elphick, **Structural analysis of the starfish SALMFamide neuropeptides S1 and S2: the N-terminal**

region of S2 facilitates self-association. Biochim. Biophys. Acta., 1844 (2014): pp. 358-65.DOI: 10.1016/j.bbapap.2013.10.013.

16. Jones, C.E., C.B. Otara, N.D. Younan, J.H. Viles, and M.R. Elphick, **Bioactivity and structural properties of chimeric analogs of the starfish SALMFamide neuropeptides S1 and S2**. Biochim. Biophys. Acta., 1844 (2014): pp. 1842-50.DOI: 10.1016/j.bbapap.2014.08.001.

17. Elphick, M.R., D.C. Semmens, L.M. Blowes, J. Levine, C.J. Lowe, M.I. Arnone, and M.S. Clark, **Reconstructing SALMFamide Neuropeptide Precursor Evolution in the Phylum Echinodermata: Ophiuroid and Crinoid Sequence Data Provide New Insights**. Front. Endocrinol. (Lausanne), 6 (2015): pp. 2. DOI: 10.3389/fendo.2015.00002.

18. Elphick, M.R., S. Achhala, and N. Martynyuk, **The evolution and diversity of SALMFamide neuropeptides**. PLoS One, 8 (2013): pp. e59076.DOI: 10.1371/journal.pone.0059076.

19. Bather, F.A., *The Echinodermata*, in *A treatise on zoology, part III, A and C.*, R.R. Lankester, Editor. 1900, Black: London.

20. Mooi, R. and B. David, **What a new model of skeletal homologies tells us about asteroid evolution**. American Zoologist, 40 (2000): pp. 326-339.DOI: Doi 10.1668/0003-1569(2000)040[0326:Wanmos]2.0.Co;2.

21. Janies, D. and R. Mooi, *Xyloplax is an asteroid.*, in *Echinoderm Research*, M. Candia Carnevali and F. Bonasoro, Editors. 1998, Balkema: Rotterdam. p. 311-316.

22. Janies, D., **Phylogenetic relationships of extant echinoderm classes**. Canadian Journal of Zoology-Revue Canadienne De Zoologie, 79 (2001): pp. 1232-1250.DOI: DOI 10.1139/cjz-79-7-1232.

23. Telford, M.J., C.J. Lowe, C.B. Cameron, O. Ortega-Martinez, J. Aronowicz, P. Oliveri, and R.R. Copley, **Phylogenomic analysis of echinoderm class relationships supports Asterozoa**. Proc. Biol. Sci., 281 (2014).DOI: Doi 10.1098/Rspb.2014.0479.

24. O'Hara, T.D., A.F. Hugall, B. Thuy, and A. Moussalli, **Phylogenomic Resolution of the Class Ophiuroidea Unlocks a Global Microfossil Record**. Curr. Biol., 24 (2014): pp. 1874-1879.DOI: DOI 10.1016/j.cub.2014.06.060.

25. Reich, A., C. Dunn, K. Akasaka, and G. Wessel, **Phylogenomic Analyses of Echinodermata Support the Sister Groups of Asterozoa and Echinozoa**. Plos One, 10 (2015).DOI: DOI 10.1371/journal.pone.0119627.

26. Cannon, J.T., K.M. Kocot, D.S. Waits, D.A. Weese, B.J. Swalla, S.R. Santos, and K.M. Halanych, **Phylogenomic Resolution of the Hemichordate and Echinoderm Clade**. Curr. Biol., 24 (2014): pp. 2827-2832.DOI: DOI 10.1016/j.cub.2014.10.016.

27. Yun, S.S., M.C. Thorndyke, and M.R. Elphick, **Identification of novel SALMFamide neuropeptides in the starfish *Marthasterias glacialis***. Comp. Biochem. Physiol. A Mol. Integr. Physiol., 147 (2007): pp. 536-42.

28. Conato, C., R. Gavioli, R. Guerrini, H. Kozlowski, P. Mlynarz, C. Pasti, F. Pulidori, and M. Remelli, **Copper complexes of glycyl-histidyl-lysine and two of its synthetic analogues: chemical behaviour and biological activity**. Biochim. Biophys. Acta., 1526 (2001): pp. 199-210.DOI: 10.1016/S0304-4165(01)00127-1.

29. Semmens, D.C., R.E. Dane, M.R. Pancholi, S.E. Slade, J.H. Scrivens, and M.R. Elphick, **Discovery of a novel neurophysin-associated neuropeptide that triggers cardiac stomach contraction and retraction in starfish**. J. Exp. Biol., 216 (2013): pp. 4047-53.DOI: 10.1242/jeb.092171.

30. Haas, B.J., A. Papanicolaou, M. Yassour, M. Grabherr, P.D. Blood, J. Bowden, M.B. Couger, D. Eccles, B. Li, M. Lieber, M.D. MacManes, M. Ott, J. Orvis, N. Pochet, F. Strozzi, N. Weeks, R. Westerman, T. William, C.N. Dewey, R. Henschel, R.D.

Leduc, N. Friedman, and A. Regev, **De novo transcript sequence reconstruction from RNA-seq using the Trinity platform for reference generation and analysis**. Nature Protocols, 8 (2013): pp. 1494-1512.DOI: DOI 10.1038/nprot.2013.084.

31.   Stoll, S. and A. Schweiger, **EasySpin, a comprehensive software package for spectral simulation and analysis in EPR**. J. Magn. Reson., 178 (2006): pp. 42-55.DOI: 10.1016/j.jmr.2005.08.013.

32.   Froncisz, W. and J.S. Hyde, **Broadening by strains of lines in the g-parallel region of Cu2+ EPR spectra.** J. Chem. Phys., 73 (1980): pp. 3123 - 3131.DOI: 10.1063/1.440548.

33.   Marat, K., *SpinWorks 4.1.0*. 2014, University of Manitoba: Canada.

34.   Lever, A.B.P., *Inorganic Electronic Spectroscopy*. 1984, New York: Elsevier.

35.   Stanyon, H.F., X. Cong, Y. Chen, N. Shahidullah, G. Rossetti, J. Dreyer, G. Papamokos, P. Carloni, and J.H. Viles, **Developing predictive rules for coordination geometry from visible circular dichroism of copper(II) and nickel(II) ions in histidine and amide main-chain complexes**. FEBS J., 281 (2014): pp. 3945-54.DOI: 10.1111/febs.12934.

36.   Hureau, C., H. Eury, R. Guillot, C. Bijani, S. Sayen, P.L. Solari, E. Guillon, P. Faller, and P. Dorlet, **X-ray and solution structures of Cu(II) GHK and Cu(II) DAHK complexes: influence on their redox properties**. Chemistry, 17 (2011): pp. 10151-60.DOI: 10.1002/chem.201100751.

37.   Trapaidze, A., C. Hureau, W. Bal, M. Winterhalter, and P. Faller, **Thermodynamic study of Cu2+ binding to the DAHK and GHK peptides by isothermal titration calorimetry (ITC) with the weaker competitor glycine**. J. Biol. Inorg. Chem., 17 (2012): pp. 37-47.DOI: 10.1007/s00775-011-0824-5.

38.   Peisach, J. and W.E. Blumberg, **Structural implications derived from the analysis of electron paramagnetic resonance spectra of natural and artificial copper proteins**. Arch. Biochem. Biophys., 165 (1974): pp. 691-708.DOI: 10.1016/0003-9861(74)90298-7.

39.   Bonomo, R.P., V. Cucinotta, A. Giuffrida, G. Impellizzeri, A. Magri, G. Pappalardo, E. Rizzarelli, A.M. Santoro, G. Tabbi, and L.I. Vagliasindi, **A re-investigation of copper coordination in the octa-repeats region of the prion protein**. Dalton Trans., (2005): pp. 150-8.DOI: 10.1039/b415727c.

40.   Hyde, J.S., B. Bennett, E.D. Walter, G.L. Millhauser, J.W. Sidabras, and W.E. Antholine, **EPR of Cu2+ prion protein constructs at 2 GHz using the g(perpendicular) region to characterize nitrogen ligation**. Biophys. J., 96 (2009): pp. 3354-62.DOI: 10.1016/j.bpj.2009.01.034.

41.   Michael, J.P. and G. Pettenden, **Marine metabolites and metal ion chelation: The facts and the fantasies.** Angew. Chem. Int. Ed. Engl., 32 (1993): pp. 1-23.

42.   Kogut, M.B. and B.M. Voelker, **Strong copper-binding behavior of terrestrial humic substances in seawater**. Environ. Sci. Technol., 35 (2001): pp. 1149-56.DOI: 10.1021/es0014584.

43.   Ndungu, K., **Model predictions of copper speciation in coastal water compared to measurements by analytical voltammetry**. Environ. Sci. Technol., 46 (2012): pp. 7644-52.DOI: 10.1021/es301017x.

44.   Satani, M., K. Takahashi, H. Sakamoto, S. Harada, Y. Kaida, and M. Noguchi, **Expression and characterization of human bifunctional peptidylglycine alpha-amidating monooxygenase**. Protein Expr. Purif., 28 (2003): pp. 293-302.DOI: 10.1016/S1046-5928(02)00684-8.

45.   Harrison, M.D., C.E. Jones, M. Solioz, and C.T. Dameron, **Intracellular copper routing: the role of copper chaperones**. Trends Biochem. Sci., 25 (2000): pp. 29-32.DOI: DOI:10.1016/S0968-0004(99)01492-9.

46.   Herman, A., H. Kozlowski, M. Czauderna, K. Kochman, K. Kulon, and A. Gajewska, **Gondaoliberin (GnRH) and its copper complex (Cu-GnRH) enzymatic degradation in hypothalmic and pituitary tissue in vitro.** J. Physiol. Pharmacol, 63 (2012): pp. 69-75.

47.   Ruppert, E.E., R.S. Fox, and R.D. Barnes, *Invertebrate Zoology: A Functional Evolutionary Approach.* 7th ed. 2003, Belmont, CA: Brooks Cole Thompson.

Figure Legends

Figure 1. C-terminally aligned sequences of SALMFamide neuropeptides derived from L-type SALMFamide precursors in the Asteroidea (*Patiria miniata*, *Asterias rubens* and *Remaster gourdoni*) [1], Ophiuroidea (*Ophionotus victoriae*, *Ophioderma brevispinum* and *Ophiothrix angulata* [2], Echinoidea (*Strongylocentrotus purpuratus*, *Arbacia punctulata* and *Eucidaris tribuloides*) [3] and Holothuroidea (*Apostichopus japonicus*, *Psolus spp* and *Pannychia moseleyi*) [4]. The third amino acid residue from the C-terminal amide has been highlighted in red if it is leucine or isoleucine, yellow if phenylalanine or tyrosine and grey if any other residue. Histidine residues located in the sixth position from C-terminal amide have been highlighted in turquoise.

Figure 2. C-terminally aligned sequences of SALMFamide neuropeptides derived from from F-type SALMFamide precursors in the Asteroidea (*Patiria miniata*, *Asterias rubens* and *Remaster gourdoni*) [1], Ophiuroidea (*Ophionotus victoriae*, *Astrophyton muricatum* and *Ophiothrix angulata* [2], Echinoidea (*Strongylocentrotus purpuratus*, *Arbacia punctulata* and *Lytechinus variegatus*) [3] and Holothuroidea (*Apostichopus japonicus*, *Psolus spp* and *Stichopus chloronatus*) [4]. The third amino acid residue from the C-terminal amide has been highlighted in red if it is leucine or isoleucine, yellow if phenylalanine or tyrosine and grey if any other. Histidine residues located in the sixth position from C-terminal amide have been highlighted in turquoise.

Figure 3. SALMFamide neuropeptides derived from SALMFamide precursors in the Crinoidea (*Antedon mediterranea, Isometra vivipara* and *Oligometra serripinna*). The third amino acid residue from the C-terminal amide has been highlighted in red if it is leucine or isoleucine, yellow if phenylalanine or tyrosine and grey if any other residue. Histidine located in the sixth position from C-terminal amide residues have been highlighted in turquoise.

Figure 4. Copper(II) and nickel(II) titrations monitored by electronic spectroscopy.

32

(A) Titration of Cu^{2+} (solid black line) into AYHSALPF-NH_2 (100 μM, 10 mM nEM, pH 7.44) results in the formation of a peak at 520 nm. Titration of Ni^{2+} (dashed red line) results in an increase in absorption at 420 nm. (B) Plots of the absorbance at 520 nm (Cu^{2+}) and 420 nm (Ni^{2+}) as a function of added metal. Both curves plateau around 100 μM metal, suggesting 1:1 stoichiometry. (C) Titration of Cu^{2+} (solid black line) and Ni^{2+} (dashed red line) into GYHSGLPF-NH_2 (80 μM, 10 mM nEM, pH 7.44) results in the formation of peaks at 520 nm and 420 nm, respectively. (D) Plots of the absorbance at 520 nm (Cu^{2+}) and 420 nm (Ni^{2+}) as a function of added metal. Both curves plateau around 80 μM metal, suggesting 1:1 stoichiometry. (E) Titration of Cu^{2+} into LHSALPF-NH_2 (110 μM, 10 mM nEM, pH 7.44) generates an absorption band at 600 nm and the binding curve (F) suggests a stoichiometry of 1:1.

Figure 5. Paramagnetic copper causes broadening of GYHSGLPF-NH_2 and LHSALPF-NH_2 ^1H NMR spectra. (A) ^1H NMR spectra of ~500 μM apo-GYHSGLPF- NH_2 in 10% D_2O/90% H_2O, pH 7.2 (bottom trace) and after the addition of 0.1 equivalent Cu^{2+} (top trace). Assignment of selected perturbed peaks is shown in top trace. (B). ^1H NMR spectra of ~500 μM apo-LHSALPF- NH_2 in 10% D_2O/90% H_2O, pH 7.2 (bottom trace) and after the addition of 0.1 equivalent Cu^{2+} (top trace). Assignment of selected perturbed peaks is shown in top trace. Expansion of assigned peaks in both A and B are shown in supplementary material figure S3.

Figure 6. Copper(II) titrations monitored by circular dichroism spectroscopy. (A) CD spectra (300 – 700 nm) were collected as Cu^{2+} was titrated into apo-GYHSGLPF-NH_2 (93 μM, 10 mM nEM, pH 7.7). Peaks at 490 nm and 570 nm are due to d-d transitions and the peak in the near-UV (316 nm) can be attributed to an amide $N^- \rightarrow$ Cu(II) CT. (B) The intensity of the peaks at 316 nm (■) and 490 nm (●) plotted as a function of [Cu(II)]/[GYHSGLPF-NH_2] plateaus at a ratio near one. (C) CD spectra obtained during a titration of apo-LHSALPF-NH_2

(96 μM, 10 mM nEM, pH 7.7) with Cu^{2+} show low intensity peaks at 300 nm (amide N→

Cu(II) CT), 346 nm (imidazole N→ Cu^{2+} CT) and 600 nm (d-d transition). (D) The intensity

of the peaks at 300 nm (■) and 346 nm (●) plotted as a function of [Cu(II)]/[LHSALPF-NH_2]

plateaus at a ratio near one.

Figure 7. X-band EPR spectra of Cu^{II}-bound peptides. (A) First derivative spectrum of

[Cu^{II}(GYHSGLPF-NH_2)] (ν = 9.433547, 262 μM, 10 mM nEM, pH 7.2, 0.98 equivalents

Cu^{2+}), dashed line is simulated spectrum, (B) first derivative spectrum of [Cu^{II}(LHSALPF-

NH_2)] (ν = 9.433526, 1 mM, 10 mM nEM, pH 7.2, 0.96 equivalents Cu^{2+}), (C) first

derivative spectrum of a mixture of [Cu^{II}(LHSALPF-NH_2)] (ν = 9.432792, 260 μM, 10 mM

nEM, pH 7.2) and apo-GYHSGLPF-NH_2 (243 μM,10 mM nEM, pH 7.2). Inset (c) shows the

second derivative spectrum of (C) highlighting the perpendicular region (exp), along with the

same region after simulation assuming four (4N) or three (3N) nitrogen donors. (D) Titration

of Cu^{2+} into LHSALPF-NH_2 (110 μM, 10 mM nEM, pH 7.44) generates an absorption band

at 600 nm. Leaving the sample at room temperature for 2 hrs generated a spectrum with

broadened d-d transitions.

Figure 8. The occurrence and properties of SALMFamide precursors in species representing

each of the five extant echinoderm classes. *A. rub* is the starfish *Asterias rubens* (Asteroidea),

O. vic is the brittlestar *Ophionotus victoriae* (Ophiuroidea), *S. pur* is the sea urchin

Strongylocentrotus purpuratus (Echinoidea), *A. jap* is the sea cucumber *Apostichopus*

japonicus (Holothuroidea) and *A. med* is the feather star *Antedon mediterranea* (Crinoidea).

Signal peptides are shown in blue, spacer peptides are in white, monobasic or dibasic

cleavage sites are in green, SALMFamides with a C-terminal FXXamide motif are in yellow,

a LXXamide motif are in red and a XXXamide motif are in grey. In addition, SALMFamides

containing a histidine residue at the sixth position from the C-terminal amide are marked with

H and peptides in which this histidine residue forms an ATCUN motif have been marked

with an asterisk. The data indicate that the common ancestor of all extant echinoderms had a

single SALMFamide precursor, including histidine-containing L-type SALMFamides, as in

extant crinoids. Then duplication (x2) of the SALMFamide precursor in the common ancestor

of extant Eleutherozoa followed by divergence gave rise to two types of precursor: the L-type

precursor, which typically includes SALMFamides with a conserved histidine residue, and

the F-type precursor. Figure modified from Elphick et al. [17].

Table 1. Spin Hamiltonian parameters for Cu^{II}SALMFamide peptides.

Complex	g_x	g_y	g_z	A_x (^{63}Cu)[a]	A_y (^{63}Cu)[a]	A_z (^{63}Cu)[a]
$[Cu^{II}(GYHSGLPF-NH_2)]$	2.044	2.044	2.176	22.1	22.1	200.9
$[Cu^{II}(LHSALPF-NH_2)]$	2.042	2.042	2.220	-	-	187.5
$[Cu^{II}(LHSALPF-NH_2)$ + apoGYHSGLPF-NH$_2$	2.045	2.067	2.207	11.5	12.1	197.3

a. units 10^{-4} cm^{-1}

Identification of a neuropeptide precursor protein that gives rise to a "cocktail" of peptides that bind Cu(II) and generate metal-linked dimers

Christopher E. Jones[a⊥*], Meet Zandawala[b⊥], Dean C. Semmens[b], Sarah Anderson[b],

Graeme R. Hanson[c‖], Daniel A. Janies[d] and Maurice R. Elphick[b*]

[a.]School of Science and Health, Western Sydney University, Locked bag 1797,

Penrith, 2751, New South Wales, Australia.

[b.]School of Biological & Chemical Sciences, Queen Mary University of London,

Mile End Road, London, E1 4NS, UK.

[c.] Centre for Advanced Imaging, The University of Queensland, Brisbane,

Queensland, 4072, Australia

[d.]Department of Bioinformatics and Genomics, University of North Carolina at Charlotte,

Charlotte, NC 28223 USA

*To whom correspondence should be addressed:

Christopher E. Jones, School of Science and Health, Western Sydney University, Locked bag

1797, Penrith, NSW, 2759, Australia. Tel: +61 29685 9908; Fax: +61 2 9685 9915; E-mail:

c.jones@uws.edu.au

or

Maurice R. Elphick, School of Biological & Chemical Sciences, Queen Mary University of

London, Mile End Road, London, E1 4NS, UK. Tel: 0207 882 6664; Fax: 0207 882 7732; E-

mail: m.r.elphick@qmul.ac.uk

⊥ These authors contributed equally.

‖ Deceased, 16/07/1955 – 25/02/2015

Abstract

Background

Neuropeptides with an Amino Terminal Cu(II), Ni(II) Binding (ATCUN) motif (H_2N-xxH) bind Cu(II)/Ni(II) ions. Here we report the novel discovery of a neuropeptide precursor that gives rise to a "cocktail" of peptides that bind Cu(II)/Ni(II) and form ternary complexes – the L-type SALMFamide precursor in the starfish *Asterias rubens*.

Methods

Echinoderm transcriptome sequence data were analysed to identify transcripts encoding precursors of SALMFamide-type neuropeptides. The sequence of the L-type SALMFamide precursor in the starfish *Asterias rubens* was confirmed by cDNA sequencing and peptides derived from this precursor (e.g. AYHSALPF-NH_2, GYHSGLPF-NH_2 and LHSALPF-NH_2) were synthesised. The ability of these peptides to bind metals was investigated using UV/Vis, NMR, circular dichroism and EPR spectroscopy.

Results

AYHSALPF-NH_2 and GYHSGLPF-NH_2 bind Cu(II) and Ni(II) and generate metal-linked dimers to form ternary complexes with LHSALPF-NH_2. Investigation of the evolutionary history of the histidine residue that confers these properties revealed that it can be traced to the common ancestor of echinoderms, which is estimated to have lived ~500 million years ago. However, L-type precursors comprising multiple SALMFamides with the histidine residue forming an ATCUN motif appears to be a feature that has evolved uniquely in starfish (Asteroidea).

General Significance

The discovery of a SALMFamide-type neuropeptide precursor protein that gives rise to a "cocktail" of peptides that bind metal ions and generate metal-linked dimers provides a new insight on ATCUN motif-containing neuropeptides. This property of L-type SALMFamides

in the Asteroidea may be associated with a role in regulation of the unusual extra-oral feeding behavior of starfish.

1.0 Introduction

Neuropeptides are neuronal intercellular signalling molecules that act as neurotransmitters, neuromodulators or neurohormones and regulate many physiological processes and behaviours in humans and other animals [1]. They are derived from larger precursor proteins and are subject to post-translational modifications that are important for function; for example, in many neuropeptides a C-terminal glycine residue is converted to an amide group. Furthermore, in some neuropeptides the presence of a histidine residue can confer the ability to bind metal ions. In particular, the presence of an Amino Terminal Cu(II), Ni(II) Binding (ATCUN) motif, where a histidine residue is specifically located in the third position from the N-terminus (i.e. H_2N-xxH, where x is variable), has been found to confer high affinity binding of Cu(II) and Ni(II). The ATCUN motif was originally characterized in albumins but subsequently it has been demonstrated that other peptides/proteins with an ATCUN motif also bind Cu(II) and/or Ni(II) ions [2, 3]. In 1995 Harford and Sarkar demonstrated that the mammalian neuropeptide neuromedin C, which has the N-terminal sequence Gly-Asn-His, binds both Cu(II) and Ni(II) specifically. Furthermore, the authors speculated that this property of neuromedin C may have relevance to neurological deficits associated with copper metabolism disorders, such as Menkes disease and Wilson disease [4]. More recently, Russino et al. reported that the mammalian tachykinin-type peptide neurokinin B, which contains an ATCUN motif, binds Cu(II) ions in an unusual $[Cu^{II}(NKB)_2]$ complex [5]. Furthermore, although Cu(II) binding substantially alters the structure of neurokinin B, the ability of $[Cu^{II}(NKB)_2]$ to activate the NKB receptor was not impeded. It was speculated that NKB may have a role in protecting cells from the effects of neuronally released copper. Several other members of the tachykinin peptide family have also been shown to coordinate copper ions, yet the physiological consequences remain to be determined [6, 7].

Here we report the novel discovery of a neuropeptide precursor protein that gives rise to a "cocktail" of neuropeptides that bind Cu(II) – the starfish L-type SALMFamide precursor. SALMFamide neuropeptides occur in species belonging to the phylum Echinodermata, which includes starfish, brittle stars, sea urchins, sea cucumbers and feather stars [8]. The first members of this neuropeptide family to be identified, S1 and S2, were both isolated from the starfish species *Asterias rubens* and *Asterias forbesi*. S1 is an octapeptide with the amino acid sequence GFNSALMF-NH$_2$ and S2 is a dodecapeptide with the amino acid sequence SGPYSFNSGLTF-NH$_2$ [9, 10]. Subsequently, SALMFamides were identified in other echinoderms, including GFSKLYF-NH$_2$ and SGYSVLYF-NH$_2$ from the sea cucumber *Holothuria glaberrima* and GYSPFMF-NH$_2$ and FKSPFMF-NH$_2$ from the sea cucumber *Apostichopus japonicus* [11]. Identification of these holothurian neuropeptides revealed the existence of two types of SALMFamides. Firstly, L-type SALMFamides that have the C-terminal motif SxLxF-NH$_2$ (e.g. S1, S2, GFSKLYF-NH$_2$ and SGYSVLYF-NH$_2$) and secondly, F-type SALMFamides that have the C-terminal motif SxFxF-NH$_2$ (GYSPFMF-NH$_2$ and FKSPFMF-NH$_2$).

Investigation of the bioactivity of SALMFamides in echinoderms has revealed that both L-type and F-type SALMFamides act as muscle relaxants [12]. For example, S1 and S2 both cause dose-dependent relaxation of apical muscle, tube foot and cardiac stomach preparations from the starfish *A. rubens* [13, 14]. Furthermore, S2 exhibits higher potency/efficacy than S1, which provided a rationale for investigation of a structural basis for this difference in bioactivity. By testing chimeric analogs of S1 and S2, it was found that it is the C-terminal region of the peptides that is the primary determinant of their differing potency/efficacy [15, 16]. However, the N-terminal tetrapeptide (SGPY) of S2 contributes to its bioactivity and confers on S2 the property to self-associate and form highly structured multimers at high concentrations [15]. Interestingly, addition of the SGPY tetrapeptide to the

N-terminus of S1 confers structure that is not observed with the S1 peptide, but without enhancing bioactivity. Thus, the differing bioactivity of S1 and S2 is determined by a complex interplay of sequence and conformation.

Advances in genome/transcriptome sequencing have enabled determination of the sequences of SALMFamide neuropeptide precursor proteins. For example, sequencing of the genome and transcriptome of the starfish *Patiria miniata* revealed: 1) an "L-type" precursor comprising S1 and six other L-type SALMFamides and 2) an "F-type" precursor comprising eight F-type or F-type-like SALMFamides and an S2-like peptide (L-type). Furthermore, comparative analysis of sequence data from a variety of echinoderm species has enabled investigation of the evolution of SALMFamide precursors [17, 18]. The phylum Echinodermata comprises five extant classes, Asteroidea (starfish), Ophiuroidea (brittle stars), Echinoidea (sea urchins, sand dollars), Holothuroidea (sea cucumbers) and Crinoidea (feather stars and sea lilies), and the phylogenetic relationships of these classes have been determined. Thus, the Asteroidea and Ophiuroidea are sister classes (the Asterozoa) and the Echinoidea and Holothuroidea are sister classes (the Echinozoa), with the Crinoidea basal to the Asterozoa and Echinozoa [19-26]. This phylogeny has provided a framework to reconstruct the evolution of SALMFamide precursors in the phylum Echinodermata. In crinoid species only a single SALMFamide precursor has been identified, whereas asterozoan and echinozoan species have both an L-type and an F-type precursor. It has therefore been postulated that the L-type and F-type precursors found in asterozoans and echinozoans may have arisen by duplication of a common ancestral-type precursor similar to that found in extant crinoids [17].

Here we have obtained additional sequences of SALMFamide precursors in echinoderm species representing the five extant classes. Comparative analysis of the sequences of echinoderm SALMFamide precursors revealed that several neuropeptides

derived from L-type SALMFamide precursors in starfish have an ATCUN motif. For example AY<u>H</u>SALPF-NH$_2$, a neuropeptide that has been identified previously in the starfish species *Marthasterias glacialis* [27]. In addition, one of the peptides derived from L-type SALMFamide precursors in starfish (e.g. LHSALPF-NH$_2$) has a histidine in the same position as the tripeptide Gly-His-Lys (GHK), a well-studied naturally occurring human copper-binding growth factor [28]. We show here that L-type SALMFamides in the starfish *A. rubens* that have an ATCUN motif are able to bind Cu(II) and Ni(II). Furthermore, Cu(II) binding to these peptides facilitates formation of ternary complexes with LHSALPF-NH$_2$. The evolutionary and functional significance of these properties of neuropeptides derived from the L-type SALMFamide precursor in starfish is discussed.

2.0 Materials and Methods

2.1 Transcriptome sequencing

The sequences of SALMFamide precursors have been determined in species representing all five echinoderm classes, as reported previously [17, 18]. Here we have obtained additional transcriptome sequence data from other species belonging to each of the five echinoderm classes: the starfishes *Asterias rubens* and *Remaster gourdoni* (class Asteroidea), the brittle stars *Ophioderma brevispinum* and *Astrophyton muricatum* (class Ophiuroidea), the sea urchins *Arbacia punctulata* and *Eucidaris tribuloides* (class Echinoidea), the sea cucumbers *Psolus spp*, *Stichopus chloronatus* and *Pannychia moseleyi* (class Holothuroidea) and the feather stars *Isometra vivipara* and *Oligometra serripinna* (class Crinoidea).

Asterias rubens radial nerve cord transcriptome sequence data were obtained as reported previously [29]. For the other echinoderm species, RNA was extracted from tube feet (*Remaster gourdoni*), arms (*Ophioderma brevispinum*, *Astrophyton muricatum*), body wall (*Arbacia punctulata*, *Eucidaris tribuloides*, *Psolus spp*, *Stichopus chloronatus*, *Pannychia moseleyi*) or pinnules (*Isometra vivipara*, *Oligometra serripinna*) and then subjected to RNA-Seq sequencing on an Illumina Hiseq 2000 platform (100 base pairs, paired end). Reads for each of the samples were filtered by quality score (cutoff threshold > Q20) using fastxtrimmer and Illumina adapters were removed using fastxclipper, which are both components of the fastx toolkit (http://hannonlab.cshl.edu/fastx_toolkit/). *De novo* assembly of contigs was then performed using Trinity on a high memory computer cluster using 500 GB of RAM and 24 CPUs [30].

2.2 Cloning and sequencing of the L-type SALMFa precursor cDNA from *A. rubens*

SALMFamides derived from the *A. rubens* L-type SALMFamide precursor were selected for the metal-binding studies described below. To facilitate this it was first necessary to confirm, by cDNA cloning and sequencing, the sequence of the precursor predicted from Illumina transcriptome sequencing. Total RNA from radial nerve cords of *A. rubens* was isolated using the Total RNA Isolation System (Promega) and used for cDNA synthesis using the Quantitect Reverse Transcription Kit (QIAgen). The full-length cDNA of the *A. rubens* L-type SALMFa precursor, including 5′ and 3′ untranslated regions (UTR), was amplified by PCR using Phusion high-fidelity PCR master mix (NEB) and the oligos 5′-TAGCTACTTGACACA-3′ and 5′-ATATGACTAGTTGAGAGAGG-3′, which were designed using Primer3 software (http://bioinfo.ut.ee/primer3-0.4.0/). The PCR product was gel-extracted and purified using a QIAquick gel extraction kit (QIAgen) before being blunt-end cloned into a pBluescript SKII (+) vector (Agilent Technologies) cut with a *Eco*RV-HF restriction endonuclease (NEB). The clone was then sequenced (Eurofins Genomics) from the T7 and pCR3.1-BGH-rev sequencing primer sites.

2.3 Neuropeptide synthesis and metal titrations

The *A. rubens* L-type SALMFamides AYHSALPF-NH$_2$, GYHSGLPF-NH$_2$ and LHSALPF-NH$_2$ were synthesised by Synpeptide (Shanghai, China) and were >95% pure as determined by mass spectrometry and NMR. The lyophilized peptides were weighed and dissolved in the required buffer (10 mM nEM unless otherwise stated) on the day of use. The peptide concentration was estimated using the extinction coefficient of the single tyrosine amino acid (ε_{280nm} = 1280 M^{-1}cm^{-1}) or from the measured mass taking into consideration the presence of ~30% water. Stock (0.5 M) solutions of copper and nickel were prepared as CuCl$_2 \cdot$2H$_2$O and NiCl$_2 \cdot$2H$_2$O in water and diluted to working solutions on the day of use.

9

Metal addition during titrations was achieved using a 10 μL Hamilton gastight syringe. The spectrum of metal-free peptide was subtracted from the spectrum after each metal addition and dilution effects were taken into account during processing of the spectra.

2.4 Electronic Spectroscopy

UV/Visible electronic spectra (300 nm – 700 nm) were acquired on a Perkin-Elmer U-3100 using a 10 mm pathlength cuvette.

2.5 Circular dichroism (CD) Spectroscopy

CD spectra were collected on a Jasco J810 spectrometer. Spectra were routinely collected over the range 300 nm to 700 nm using a 10 mm cuvette with sampling every 1 nm. A minimum of 10 spectra were obtained and averaged, prior to smoothing using an 11-point moving average method in the Jasco software.

2.6 Electron Paramagnetic Resonance (EPR) Spectroscopy

Continuous wave EPR spectra at ~9.4 GHz (X-band) were obtained on a Bruker Elexsys E500 spectrometer operated with Bruker Xepr software and equipped with a super high-Q cavity. Calibration of the field was achieved using an ER036TM teslameter and the microwave frequency was calibrated with an EIP548B frequency counter. Stable temperatures of $150 \pm 5K$ were achieved using a nitrogen gas flow through system linked to a Eurotherm B-VT-2000 variable temperature controller. Instrument settings were: modulation frequency 100 kHz; modulation amplitude 0.63G; microwave power $10 - 20$ mW; number of scans $40 - 60$; time constant 5.12 ms; sweep time 84 s. Spectra were baseline corrected using a polynomial function and high frequency noise was removed using Fourier filtering available in the Xepr software. Spectra were simulated using the least-squares fitting

algorithm in Easyspin running in Matlab R2014a [31]. The copper hyperfine and Zeeman

interactions were initially simulated using matrix diagonalization, and perturbation theory

was used after inclusion of nitrogen nuclei to simulate the nitrogen superhyperfine

interactions. Where the presence of multiple absorbing species was apparent (i.e.

[Cu^{II}LHSALPF-NH$_2$]) the magnetic parameters were estimated directly from the spectrum.

Linewidths were fit using a correlated distribution of g- and A-values [32].

2.7 Nuclear Magnetic Resonance (NMR) Spectroscopy

NMR spectra were acquired on a Bruker Avance 500 MHz spectrometer equipped with a 5

mm TXI BBI probe and controlled using TopSpin 2.1 (Bruker Biospin, Germany). Samples

were prepared in 90% H$_2$O/10% D$_2$O and the pH was adjusted using aliquots of concentrated

HCl or NaOH. Proton spectra were acquired over a 10 ppm spectral width comprising 64K

complex points, and the residual water signal was supressed using a W5 watergate sequence.

Spectra were processed using a $\pi/2$ shifted sine squared window function in SpinWorks 4

[33].

3.0 Results

3.1 Identification of novel SALMFamide precursor sequences

Sequences encoding SALMFamide precursors have been identified previously in species representing each of the five classes in Echinodermata [17, 18]. These include sequences from *Patiria miniata* (Class Asteroidea; Order Valvatida), *Luidia senegalensis* (Class Asteroidea; Order Paxillosida), *Ophionotus victoriae* (Class Ophiuroidea; Order Ophiurida), *Ophiothrix angulata* (Class Ophiuroidea; Order Ophiurida), *Strongylocentrotus purpuratus* (Class Echinoidea; Order Echinoida), *Lytechinus variegatus* (Class Echinoidea; Order Temnopleuroida), *Apostichopus japonicus* (Class Holothuroidea; Order Aspidochirotida), *Leptosynapta tenuis* (Class Holothuroidea; Order Apodida) and *Antedon mediterranea* (Class Crinoidea; Order Comatulida) and *Aporometra wilsoni* (Class Crinoidea; Order Comatulida).

Here, by analysis of new transcriptome sequence data, we have identified SALMFamide precursors in other echinoderm species, which include *Asterias rubens* (Class Asteroidea, Order Forcipulatida), *Remaster gourdoni* (Class Asteroidea, Order Velatida), *Ophioderma brevispinum* (Class Ophiuroidea, Order Ophiurida), *Astrophyton muricatum* (Class Ophiuroidea, Order Euryalida), *Arbacia punctulata* (Class Echinoidea, Order Arbacioida), *Eucidaris tribuloides* (Class Echinoidea, Order Cidaroida), *Psolus spp* (Class Holothuroidea; Order Dendrochirotida), *Stichopus chloronatus* (Class Holothuroidea; Order Aspidochirotida), *Pannychia moseleyi* (Class Holothuroidea, Order Elasipodida), *Isometra vivipara* (Class Crinoidea, Order Comatulida) and *Oligometra serripinna* (Class Crinoidea, Order Comatulida).

3.2 Comparative analysis of echinoderm SALMFamide neuropeptide sequences: identification of conserved histidine residues

Determination of the sequences of SALMFamide precursors in species from each of the five echinoderm classes enabled comparison of the sequences of the constituent neuropeptides and identification of conserved characteristics. Thus, Figure 1 shows C-terminally aligned neuropeptides derived from L-type SALMFamide precursors in asterozoan and echinozoan species, with data from three species in each class shown. The presence of a leucine or an isoleucine residue (highlighted in red) in the third position from the C-terminal amide is characteristic feature of the majority of the neuropeptides, as expected for L-type SALMFamide precursor derived peptides. Furthermore, another conserved feature is the presence of a histidine residue (highlighted in turquoise) in the sixth position from the C-terminal amide, with at least one of the peptides in all but one of the twelve species having this feature. However, it is most strikingly apparent in starfish species, where six out of seven or five out of six of the SALMFamides have this characteristic. With respect to the N-terminus, the position of the conserved histidine residue is variable, ranging from position two to position eight. However, in starfish four of the five or six peptides with a histidine residue have the histidine in the third position from N-terminus. This is noteworthy because, as highlighted in the introduction, the presence of a histidine residue in this position is known to confer on peptides and proteins the ability to bind copper and nickel ions with high affinity. Hence, the H_2N-xxH motif is known as an Amino Terminal Cu(II), Ni(II) Binding (ATCUN) motif.

<<**INSERT FIGURE 1**>>

Having identified the occurrence of conserved histidine residues in SALMFamides derived from L-type precursors, we investigated if this is also a conserved feature of SALMFamides derived from F-type precursors. Thus, Figure 2 shows C-terminally aligned

neuropeptides derived from F-type SALMFamide precursors in asterozoan and echinozoan species, with data from three species in each class shown. The presence of a phenylalanine residue or a structurally similar tyrosine residue (highlighted in yellow) in the third position from the C-terminal amide is a characteristic feature of the majority of the neuropeptides, as expected for F-type SALMFamide precursor derived peptides. However, unlike in L-type SALMFamide precursor derived peptides, histidine residues are not prevalent in F-type SALMFamide precursor derived peptides (Fig. 2) and only one peptide (in the sea urchin *Arbacia punctulata*) has a histidine residue in the sixth position from the C-terminal amide.

<<**INSERT FIGURE 2**>>

Lastly, we analysed the sequences of neuropeptides derived from the singular SALMFamide precursors that have been identified in crinoids. This revealed an interesting pattern in the occurrence of histidine residues, with conserved histidines present in L-type peptides located at the extremities of the precursors. Thus, in all three crinoid species analysed here, the first and last neuropeptide in the precursor proteins is an L-type SALMFamide with a histidine residue located at the sixth position from the C-terminal amide, a feature that they share with the majority of SALMFamides derived from L-type SALMFamide precursors in asterozoan and echinozoan species (Fig. 3). By way of contrast, the twelve neuropeptides that form the core of the crinoid SALMFamide precursors mostly have phenylalanine, tyrosine or leucine residues at position three with respect to the C-terminal amide and typically do not have histidine residues. The occurrence at the extremities of crinoid SALMFamide precursors of L-type SALMFamides that have a histidine residue at position six with respect to C-terminal amide is interesting because it suggests that peptides with these characteristics may have given rise to the structurally related peptides that are

14

found in asterozoan and echinozoan L-type SALMFamide precursors. Accordingly, our data indicate that the evolutionary origin of L-type SALMFamides with a conserved histidine residue at position six with respect to the C-terminal amide can be traced back to the common ancestor of extant echinoderms. However, it is in the Asteroidea that peptides with this characteristic are most prevalent and furthermore the histidine typically occupies the third position from the N-terminus, forming a potential Cu(II) and Ni(II) binding site. This feature of SALMFamides derived from the L-type SALMFamide precursor in starfish is interesting from an evolutionary and functional perspective and therefore, as described below, we have investigated if these peptides do indeed bind Cu(II) and Ni(II) ions. To do this we synthesized and analysed neuropeptides derived from the L-type SALMFamide precursor in the common European starfish *A. rubens*.

<<**INSERT FIGURE 3**>>

3.3 Determination of the sequence of a cDNA encoding the L-type SALMFamide precursor in *A. rubens*

Cloning and sequencing of a 1028 bp cDNA encoding the *A. rubens* L-type SALMFamide precursor confirmed the predicted amino acid sequence obtained from transcriptome sequence data. Thus, the *A. rubens* L-type SALMFamide precursor is a 210 residue protein with a predicted 23-residue signal peptide and seven L-type SALMFamides that are bounded by dibasic cleavage sites (Fig. S1). Four of these peptides (AYHSALPF-NH_2, AYHTGLPF-NH_2, GYHSALPF-NH_2 and GYHSGLPF-NH_2) contain the ATCUN motif H_2N-xxH (Fig. 1 and S1). Two other peptides (PAGASAFHSALSY-NH_2 and LHSALPF-NH_2) contain a histidine residue but it is not in the third position from the N-terminus, whilst the peptide S1 (GFNSALMF-NH_2) lacks a histidine residue altogether.

15

3.4 Electronic and circular dichroism spectroscopy highlights coordination of copper and nickel to L-type SALMFamides

To investigate the copper binding ability of peptides derived from the *A. rubens* L-type SALMFamide precursor, we chose three representative peptides potentially containing copper sites: $AYHSALPF-NH_2$, $GYHSGLPF-NH_2$ and $LHSALPF-NH_2$. We initially used electronic spectroscopy to probe metal binding. Figure 4A shows the spectra obtained after titration of Cu^{2+} or Ni^{2+} into $AYHSALPF-NH_2$. Addition of Cu^{2+} to $AYHSALPF-NH_2$ gives rise to an absorption band centred on 520 nm and the intensity tends to stop increasing with copper addition at around one equivalent (Fig. 4B). An absorption maximum of 520 nm is indicative of Cu^{2+} bound with only nitrogen coordination [2]. Titration of Ni^{2+} generates an absorption band at 420 nm (Fig. 4A) and, in contrast to Cu^{2+}, the slope of the binding curve changes, rather than plateauing, at one equivalent (Fig. 4B). A peak at 420 nm is suggestive of Ni^{2+} bound in a square-planar, four-coordinate geometry [34]. Both the stoichiometry and wavelength maxima of Cu^{2+} and Ni^{2+} binding are entirely consistent with coordination of these metals to an ATCUN site. As expected, titration of these metals into $GYHSGLPF-NH_2$ produced identical results (Fig. 4C, D). The ATCUN motif generally binds copper and nickel via the N-terminal nitrogen, the histidine imidazole nitrogen, and intervening amide nitrogens (i.e. $\{N_a, 2N^-, N_{Im}\}$) and therefore the nature of the amino acid side chains is of less importance, especially in this case where only the presence of a glycine or alanine differentiates the motif in $AYHSALPF-NH_2$ and $GYHSGLPF-NH_2$. A feature of an ATCUN site is the lack of changes to the absorption maximum as a function of pH [2]. Accordingly, the maximum wavelength of $[Cu^{II}GYHSGLPF-NH_2]$ (520 nm) remains constant from $\sim$ pH 5 (Fig. S2A). In contrast to $AYHSALPF-NH_2$ and $GYHSGLPF-NH_2$, titration of Cu^{2+} into $LHSALPF-NH_2$ generates a peak at 600 nm, but, similar to the previous peptides, the absorbance plateaus at around one equivalent Cu^{2+} (Fig. 4E, F). An absorbance at 600 nm

16

suggests this peptide contains one or more oxygen ligands in its coordination sphere. A pH titration of this peptide shows the 600 nm wavelength maximum remains constant until higher pH values (> pH 9) where increasing absorption at wavelengths <600 nm suggests incorporation of an additional nitrogen donor (Fig. S2B) [28].

<<INSERT FIGURE 4>>

To further examine the copper binding sites we used NMR. The presence of low concentrations of paramagnetic Cu^{2+} tends to broaden peaks associated with protons lying within ~7Å of the metal. Addition of ~0.1 equivalent Cu^{2+} to GYHSGLPF-NH$_2$ results in selective broadening of the C_2H (7.68 ppm) and C_4H (6.92 ppm) protons of the imidazole ring (Fig. 5A) which tends to confirm His3 is a nitrogen donor. Some broadening of peaks due to the His3 Hβ protons (~3.61 ppm, shifted downfield due to ring current effects of Tyr2) is also observed (see Fig. S3 for expanded regions). Coordination of copper to the His3 amide and imidazole nitrogen ($N\delta_1$) could account for the perturbation of the beta protons. Additionally, peaks due to Tyr2 Hβ protons also show some broadening consistent with coordination to the nearby amide of Tyr2 (Fig. 5A, Fig. S3). In a similar manner addition of Cu^{2+} to LHSALPF-NH$_2$ results in a loss of peaks due to histidine imidazole protons (Fig. 5B). It is difficult to assess changes to the His3 Hβ peaks (~ 3.15 ppm, Fig. 5B) given overlap with Phe8 Hβ. A change in both the broadness and chemical shift is readily observed for the Leu1 Hβ peaks (~1.6 ppm), and to some extent the Hδ peaks (~0.9 ppm) (Fig. S3B), which suggests coordination to the nearby amide nitrogen of the amino acid. Intriguingly, despite having the same ratio of copper to peptide in both GYHSGLPF-NH$_2$ and LHSALPF-NH$_2$ the His imidazole peaks in the [Cu^{II}LHSALPF-NH$_2$] sample have completely broadened and disappeared, but remain to some extent in the [Cu^{II}GYHSGLPF-NH$_2$] sample (Fig. 5). This

suggests that the different copper-binding sites in these peptides have different copper on/off rates (on the NMR timescale) with [Cu^{II}LHSALPF-NH_2] at a comparatively faster rate than [Cu^{II}GYHSGLPF-NH_2]. The C_2H and C_4H peaks observed in the slowly exchanging [Cu^{II}GYHSGLPF-NH_2] spectrum (Fig. 5A) presumably arise from the apo form of the complex.

<<INSERT FIGURE 5>>

We next analysed the copper-complexes by circular dichroism (CD) spectroscopy. CD spectroscopy is a useful tool to analyse Cu^{2+} complexes because the d-d transitions that overlap to give a single broad peak in electronic spectroscopy can often be resolved into positive and negative peaks in CD [35]. The CD spectrum of [Cu^{II}GYHSGLPF-NH_2] is shown in Figure 6A (the spectrum of [Cu^{II}AYHSALPF-NH_2] has identical bands and is not shown). Positive bands are apparent at 316 nm and 490 nm and a weaker negative band appears at 570 nm. The bands at 490 nm and 570 nm can be attributed to d-d transitions, whereas a band around 320 nm may be attributed to an amide nitrogen $\rightarrow$ Cu^{2+} charge transfer (CT). In line with the absorption spectroscopy, the intensity of the bands tends to stop increasing at one equivalent Cu^{2+} (Fig. 6B). The visible CD spectrum of [Cu^{II}GYHSGLPF-NH_2] is strikingly similar to the copper-bound peptides GGH and DAHK, as well as that of copper-bound full length human serum albumin, suggesting similar coordination in all [35, 36]. The ATCUN motif is known to have high affinity for copper (K_d ~ 10^{-12} – 10^{-14} M) and should out-compete the weaker copper chelator glycine [37]. Titration of [Cu^{II}GYHSGLPF-NH_2] with glycine (up to 7× molar excess vs. copper) caused no apparent change to the CD spectrum of [Cu^{II}GYHSGLPF-NH_2] which tends to support binding via a high affinity ATCUN motif (data not shown). Further analysis of the copper

18

affinity of the SALMFamide peptides was not undertaken. The CD spectra obtained during a Cu^{2+} titration of LHSALPF-NH$_2$ are shown in Figure 6C. The spectra have a negative peak at 300 nm, a positive peak at 346 nm and a broad positive feature around 600 nm, and all are relatively low intensity and largely identical to the CD spectrum of [Cu^{II}GHK] [36]. The peak at 300 nm may be attributed to an amide nitrogen $\rightarrow$ Cu^{2+} CT, whereas the 346 nm peak is likely due to an imidazole nitrogen $\rightarrow$ Cu^{2+} CT, which is further supported by an absence of this peak in copper-bound tripeptides that lack a histidine [28, 35].

<<INSERT FIGURE 6>>

3.5 EPR spectroscopy predicts presence of a copper-linked ternary complex between GYHSGLPF-NH$_2$ and LHSALPF-NH$_2$.

The X-band (~9 GHz) EPR spectra of [Cu^{II}GYHSGLPF-NH$_2$] and [Cu^{II}LHSALPF-NH$_2$], each with a Cu^{2+}:peptide ratio of 0.96, are shown in Figure 7A and 7B respectively (the spectrum of [Cu^{II}AYHSALPF-NH$_2$] is identical to that of [Cu^{II}GYHSGLPF-NH$_2$] and is not shown) . The EPR spectra for both reveal an axially symmetric Cu(II) centre (i.e. $g_x = g_y \neq g_z$). For [Cu^{II}GYHSGLPF-NH$_2$] nitrogen superhyperfine (shf) coupling is apparent in the g_x, g_y (perpendicular, $g_\perp$) region between 315 – 350 mT and analysis of the characteristic parallel g_z and $A_z(^{63}Cu)$ values suggests that the copper ion is in a 4-nitrogen environment (Table 1) at this pH (7.2) [38]. In [Cu^{II}LHSALPF-NH$_2$], the peak at $g_\perp$ is considerably broadened, suggesting the presence of multiple species, however some nitrogen coupling is apparent. The presence of multiple species is supported by Cu(II) speciation studies with GHK where the presence of mono- and bis-complexes was indicated at pH values similar to those used here [3]. The parallel values (Table 1) of [Cu^{II}LHSALPF-NH$_2$] are different to those of [Cu^{II}(GYHSGLPF-NH$_2$)] and suggest inclusion of oxygen donors which has

increased g_z and decreased A_z relative to that observed for [Cu^{II}GYHSGLPF-NH$_2$]. Most likely the predominant [Cu^{II}LHSALPF-NH$_2$] species contains a CuN$_2$O$_2$ site which previous work suggests has average values of g_z = 2.238 – 2.265 and A_z = 0.0182 – 0.0187 cm^{-1} and is consistent with the electronic spectrum (Fig. 1E) [39]. When apo-GYHSGLPF-NH$_2$ is added to [Cu^{II}LHSALPF-NH$_2$] such that the peptides are equimolar (i.e. [Cu]:[total peptide] is ~0.5:1) then the spectrum in figure 7C is obtained. In this case the spectrum was best fit with Cu^{II} in a rhombically distorted environment (i.e. $g_x \neq g_y \neq g_z$). The g_z and A_z values are different to those of the pure copper-peptides and suggest that an additional nitrogen atom/s has been added to the coordination sphere [38]. Nitrogen coupling is not observed on the parallel components of the spectrum, however, compared to [Cu^{II}LHSALPF-NH$_2$] the linewidth in the perpendicular region has narrowed and the nitrogen shf coupling is more apparent. To improve resolution at $g_{x,y}$ the spectrum was differentiated and the expanded region (Fig. 7c) reveals the ^{14}N shf coupling in more detail. Theoretically, each copper hyperfine coupling is split into (2nI + 1) (I =1) lines, where n is the number of magnetically equivalent nitrogen ligands. Although it is instructive to examine the features at $g\perp$, in reality the number of lines is complicated by various factors such as the presence of multiple species, non-equivalent nitrogens and overlap with parallel features [40]. The experimental [Cu^{II}LHSALPF-NH$_2$] + apo-GYHSGLPF-NH$_2$ spectrum (Fig. 7c, exp) was fit assuming four and three nitrogens and the results (Fig. 7c 4N, 3N) suggest that the most likely coordination involves four nitrogen ligands. In neither case are the lines on the low field (320 – 325 mT) side of $g\perp$ well simulated, however on the high field side (335 – 338 mT) the four nitrogen simulation clearly fits the experimental spectrum more closely in both the line position and intensity than the three nitrogen simulation. The high field transitions are known to be particularly sensitive to the number of nitrogen ligands [40]. Thus, we predict that the predominant species formed when apo-GYHSGLPF-NH$_2$ is added to [Cu^{II}LHSALPF-NH$_2$]

has Cu^{II} in a four-nitrogen environment. The EPR spectrum does not resemble [Cu^{II}GYHSGLPF-NH$_2$] indicating that apo-GYHSGLPF-NH$_2$ has not just abstracted all the copper from [Cu^{II}LHSALPF-NH$_2$]. It is likely that the oxygen donors observed in [Cu^{II}LHSALPF-NH$_2$] have been replaced by nitrogens from apo-GYHSGLPF-NH$_2$ to form a copper-linked ternary complex. We predict that the histidine imidazole from GYHSGLPF-NH$_2$ is a nitrogen contributor the ternary complex. This result is not unprecedented, as a previous study showed addition of the amino acid histidine to a solution of [Cu^{II}GHK] generated a 4N complex where the oxygen donor in [Cu^{II}GHK] was displaced by a nitrogen from the histidine imidazole group [36]. Collection of spectra at alternative frequencies, such as S-band (~ 4 GHz) which avoids broadening due to g- and A-strain correlations, may allow nitrogen coupling to be more completely analysed.

We next wondered that if [Cu^{II}LHSALPF-NH$_2$] can form 4N complexes with apo-GYHSGLPF-NH$_2$, then why does copper titration of LHSALPF-NH$_2$ by UV/Vis spectroscopy (Fig. 4E, F) show a simple 1:1 stoichiometry with a peak at 600 nm indicative of N/O coordination, when the 4N mononuclear binary complex [Cu^{II}(LHSALPF-NH$_2$)$_2$] can presumably be formed? Given that NMR shows different copper on/off rates for the complexes then maybe the timescale of the UV/Vis experiment accounts for the observed result. To explore this [Cu^{II}LHSALPF-NH$_2$] (Fig. 7D) was scanned, left at room temperature for 2 hours then re-scanned. The resultant spectrum (Fig. 7D) shows that the d-d transitions are now much broader than in the initial sample and there is increased absorption at wavelengths shorter than 600 nm (no evidence of aggregation was observed). Taken together with the EPR data, this suggests that initially a simple [Cu^{II}LHSALPF-NH$_2$] complex with a 2N2O donor set is formed, but over time other species such as a 4N [Cu^{II}(LHSALPF-NH$_2$)$_2$] having absorption around 500 nm also occur. Along with ternary complexes, these species

21

may also contribute to the EPR spectrum (Fig. 7c) which increases the difficulty of accurately simulating the nitrogen coupling.

<<**INSERT FIGURE 7**>>

4.0 Discussion

In this study we analysed SALMFamide neuropeptide precursor sequences from species belong to the five extant classes of the phylum Echinodermata and established that peptides derived from the L-type SALMFamide precursor in starfish (class Asteroidea) were over represented with the N-terminal sequence H_2N-xxH. This sequence is a well-known copper-binding site termed an ATCUN-motif and suggested that these peptides should bind the metal. Using a range of spectroscopic techniques we show that the L-type SALMFamides in the starfish species *A. rubens* that contain the motif (e.g. GY<u>H</u>SGLPF-NH$_2$) do indeed bind Cu(II) as well as Ni(II) ions. Taken together, the spectroscopic evidence indicates Cu(II) binding to these peptides involves the His3 imidazole nitrogen, the N-terminal nitrogen and intervening amide nitrogen atoms. Ni(II) binds in a similar manner resulting in a square-planar diamagnetic complex. In addition, we show that LHSALPF-NH$_2$, a heptapeptide derived from the *A. rubens* L-type SALMFamide precursor, can also bind copper but instead of four nitrogen atoms as ligands the complex initially includes oxygen atoms. Displacement of the oxygen ligand/s in the presence of GYHSGLPF-NH$_2$ resulted in the formation of a copper-linked ternary complex (a heterodimer). To the best of our knowledge, this is the first study to report the identification of a neuropeptide precursor that contains multiple Cu(II)-binding neuropeptides.

Comparative analysis of the sequences of SALMFamide precursors in echinoderms has provided a basis for investigation of the evolutionary history of the histidine residue that

22

confers on starfish L-type precursor-derived SALMFamides the ability to bind Cu(II) ions. Crinoids, which occupy a basal position in echinoderm phylogeny, appear to have only a single SALMFamide precursor, unlike asterozoans (starfish, brittlestars) and echinozoans (sea urchins, sea cucumbers), which have an L-type and F-type SALMFamide precursor (Fig. 8). The crinoid SALMFamide precursor contains a core of twelve peptides that include F-type-like SALMFamides. However, at both the N- and C-terminal extremities of the precursor there are single L-type SALMFamides that have a histidine residue in the sixth position from the C-terminus, in common with the majority of SALMFamides derived from L-type precursors in asterozoans and echinozoans. We postulate, therefore, that following duplication of a SALMFamide precursor gene in a common ancestor of the Asterozoa and Echinozoa, one copy retained the L-type peptides with a histidine residue at position six with respect to the C-terminal amide, lost other peptides and then gave rise to the L-type SALMFamide precursors that occur in extant asterozoans and echinozoans. Conversely, the other copy retained the core peptides that do not have conserved histidine residues, lost the L-type peptides with a histidine residue at position six with respect to the C-terminal amide and then gave rise to the F-type SALMFamide precursors that occur in extant asterozoans and echinozoans. In surveying the occurrence in echinoderms of L-type SALMFamides with a histidine residue at position six with respect to the C-terminal amide, it is striking that in starfish (Asteroidea) these peptides are most abundant and have acquired the ATCUN motif by virtue of the histidine occupying the third position from the N-terminus (Fig. 8).

<<INSERT FIGURE 8>>

The concentration of free copper ions in seawater is estimated in the range of 10^{-11} – 10^{-13} M, whilst the total dissolved copper concentration, which includes organically

complexed copper, is ~ 10^{-8} M [41-43]. It is likely that the copper content of the extracellular milieu in starfish is similar to that of seawater because these animals, like other marine invertebrates, are osmoconformers. Therefore, upon release from neurons L-type SALMFamides are likely to encounter copper ions at concentrations near the K_d established for ACTUN motif-containing peptides (10^{-12} – 10^{-14} M [37]) and therefore will compete for copper ions, even when taking into consideration the ligands present in seawater which can have high binding constants [42]. Interestingly, the SALMFamides, like other amidated neuropeptides, traffic through the Golgi network where they are C-terminally amidated by the copper-metalloenzyme peptidyl-glycine alpha-amidating monooxygenase [44]. The *trans*-Golgi contains copper because several proteins are loaded with copper in this cellular compartment during their biosynthesis. Although copper is pumped into the *trans*-Golgi as Cu^+ by the Menkes ATPase [45], it is not clear whether it stays as Cu^+ or if there is some oxidation to Cu^{2+}. It is therefore interesting to speculate that, rather than being metallated after release, L-type SALMFamides containing an ATCUN motif may in fact have copper already bound to them prior to release from starfish neurons.

At the molecular level, how may the presence of bound Cu(II) ions affect the bioactivity of L-type SALMFamides? Our previous studies on the prototypical SALMFamides S1 and S2, L-type SALMFamides that do not bind metal, indicate that their bioactivity is primarily determined by the C-terminal region of the peptides. The N-terminal tetrapeptide of S2 (SGPY) does, however, influence peptide structure by causing S2 to self-associate at high concentrations and form highly-structured multimers [15]. We predicted that S2's structure and activity may change as it diffuses away from sites of release and becomes less concentrated. Further, addition of the SGPY tetrapeptide to the N-terminus of S1 confers structure on this chimeric peptide that is not observed with the S1 peptide. Now we show that the L-type SALMFamide precursor-derived peptide LHSALPF-NH$_2$ can form a copper-

linked ternary complex (a heterodimer) with GYHSGLPF-NH$_2$, and the chemistry suggests

that LHSALPF-NH$_2$ will form similar ternary complexes with any of the ATCUN-containing

L-type SALMFamides. The formation of these copper complexes (monomers and dimers)

may modify receptor binding or make the peptides more resistant to proteolysis. Interestingly,

evidence that copper binding affects enzymatic degradation of neuropeptides has been

reported recently. Herman et al. [46] reported that human gonadotropin-releasing hormone

(GnRH), which has a histidine residue at position two, binds Cu^{2+} ions and this confers on

GnRH increased resistance to enzymatic degradation in extracts of hypothalamic and

pituitary tissue. Accordingly, the copper-linked ternary complexes of LHSALPF-NH$_2$ and

ACTUN motif-containing L-type SALMFamides may likewise be more resistant to

enzymatic degradation than the monomeric peptides in the absence of copper.

At the physiological level, previous studies have revealed that SALMFamide

neuropeptides S1 and S2 cause dose-dependent relaxation of the starfish cardiac stomach *in

vitro* and trigger cardiac stomach eversion *in vivo* (Melarange et al., 1999). This

pharmacological effect of SALMFamides is of interest because starfish feed by everting their

cardiac stomach over prey and partially digesting prey tissue externally. Therefore, it is

proposed that SALMFamides may mediate neural control of cardiac stomach eversion during

starfish feeding behaviour [12]. Furthermore, extraoral feeding is unique to starfish (Class

Asteroidea) amongst extant echinoderms [47]. We speculate, therefore, that the acquisition

and proliferation of L-type SALMFamides that have an ATCUN motif and bind copper ions

in starfish may be associated with a role in regulating stomach eversion. For example, the

secretion of proteases by cells in the mucosal epithelium of the cardiac stomach during

feeding creates a proteolytic environment [47], which may have favoured acquisition of

structural characteristics that protect SALMFamides from aminopeptidases. Therefore, in this

context, our findings may provide a basis for experimental studies in which the physiological

significance of copper-binding neuropeptides could be further investigated.

Acknowledgements

References

1. Taghert, P.H. and M.N. Nitabach, **Peptide neuromodulation in invertebrate model systems**. Neuron, 76 (2012): pp. 82-97.DOI: 10.1016/j.neuron.2012.08.035.

2. Harford, C. and B. Sarkar, **Amino terminal Cu(II)- and Ni(II)-binding (ATCUN) motif of proteins and peptides: metal binding, dna cleavage, and other properties.** Acc. Chem. Res., 30 (1997): pp. 123-130.DOI: 10.1021/ar9501535.

3. Conato, C., H. Kozlowski, P. Mlynarz, F. Pulidori, and M. Remelli, **Copper and nickel complex-formation equilibria with Lys-Gly-His-Lys, a fragment of the matricellular protein SPARC**. Polyhedron, 21 (2002): pp. 1469-1474.DOI: Pii S0277-5387(02)00952-X.

4. Harford, C. and B. Sarkar, **Neuromedin C binds Cu(II) and Ni(II) via the ATCUN motif: implications for the CNS and cancer growth**. Biochem. Biophys. Res. Commun., 209 (1995): pp. 877-82.DOI: 10.1006/bbrc.1995.1580.

5. Russino, D., E. McDonald, L. Hejazi, G.R. Hanson, and C.E. Jones, **The tachykinin peptide neurokinin B binds copper forming an unusual [CuII(NKB)2] complex and inhibits copper uptake into 1321N1 astrocytoma cells**. ACS Chem. Neurosci., 4 (2013): pp. 1371-81.DOI: 10.1021/cn4000988.

6. Kowalik-Jankowska, T., E. Jankowska, Z. Szewczuk, and F. Kasprzykowski, **Coordination abilities of neurokinin A and its derivative and products of metal-catalyzed oxidation**. J. Inorg. Biochem., 104 (2010): pp. 831-42.DOI: 10.1016/j.jinorgbio.2010.03.016.

7. Pietruszka, M., E. Jankowska, T. Kowalik-Jankowska, Z. Szewczuk, and M. Smuzynska, **Complexation abilities of neuropeptide gamma toward copper(II) ions and products of metal-catalyzed oxidation**. Inorg. Chem., 50 (2011): pp. 7489-99. DOI: 10.1021/ic2002942.

8. Elphick, M.R., **SALMFamide salmagundi: The biology of a neuropeptide family in echinoderms**. Gen. Comp. Endocrinol., 205 (2014): pp. 23-35. DOI 10.1016/j.ygcen.2014.02.012.

9. Elphick, M.R., D.A. Price, T.D. Lee, and M.C. Thorndyke, **The SALMFamides: a new family of neuropeptides isolated from an echinoderm**. Proc. Bio.l Sci., 243 (1991): pp. 121-7.DOI: 10.1098/rspb.1991.0020.

10. Elphick, M.R., J.R. Reeve, Jr., R.D. Burke, and M.C. Thorndyke, **Isolation of the neuropeptide SALMFamide-1 from starfish using a new antiserum**. Peptides, 12 (1991): pp. 455-9.DOI: 10.1016/0196-9781(91)90083-2.

11. Ohtani, M., E. Iwakoshi, Y. Muneoka, H. Minakata, and K. Nomoto, **Isolation and characterization of bioactive peptides from the sea cucumber, Stichopus japonicus**. Peptide Science - Present and Future, (1999): pp. 419-420.DOI: 10.1007/0-306-46864-6_137.

12. Elphick, M.R. and R. Melarange, **Neural control of muscle relaxation in echinoderms**. J. Exp. Biol., 204 (2001): pp. 875-85.

13. Melarange, R., D.J. Potton, M.C. Thorndyke, and M.R. Elphick, **SALMFamide neuropeptides cause relaxation and eversion of the cardiac stomach in starfish.** Proc. Biol. Sci., 266 (1999): pp. 1785-1789.DOI: 10.1098/rspb.1999.0847.

14. Melarange, R. and M.R. Elphick, **Comparative analysis of nitric oxide and SALMFamide neuropeptides as general muscle relaxants in starfish**. J. Exp. Biol., 206 (2003): pp. 893-9. DOI: 10.1242/jeb.00197.

15. Otara, C.B., C.E. Jones, N.D. Younan, J.H. Viles, and M.R. Elphick, **Structural analysis of the starfish SALMFamide neuropeptides S1 and S2: the N-terminal**

region of S2 facilitates self-association. Biochim. Biophys. Acta., 1844 (2014): pp. 358-65.DOI: 10.1016/j.bbapap.2013.10.013.

16. Jones, C.E., C.B. Otara, N.D. Younan, J.H. Viles, and M.R. Elphick, **Bioactivity and structural properties of chimeric analogs of the starfish SALMFamide neuropeptides S1 and S2**. Biochim. Biophys. Acta., 1844 (2014): pp. 1842-50.DOI: 10.1016/j.bbapap.2014.08.001.

17. Elphick, M.R., D.C. Semmens, L.M. Blowes, J. Levine, C.J. Lowe, M.I. Arnone, and M.S. Clark, **Reconstructing SALMFamide Neuropeptide Precursor Evolution in the Phylum Echinodermata: Ophiuroid and Crinoid Sequence Data Provide New Insights**. Front. Endocrinol. (Lausanne), 6 (2015): pp. 2. DOI: 10.3389/fendo.2015.00002.

18. Elphick, M.R., S. Achhala, and N. Martynyuk, **The evolution and diversity of SALMFamide neuropeptides**. PLoS One, 8 (2013): pp. e59076.DOI: 10.1371/journal.pone.0059076.

19. Bather, F.A., *The Echinodermata*, in *A treatise on zoology, part III, A and C.*, R.R. Lankester, Editor. 1900, Black: London.

20. Mooi, R. and B. David, **What a new model of skeletal homologies tells us about asteroid evolution**. American Zoologist, 40 (2000): pp. 326-339.DOI: Doi 10.1668/0003-1569(2000)040[0326:Wanmos]2.0.Co;2.

21. Janies, D. and R. Mooi, *Xyloplax is an asteroid.*, in *Echinoderm Research*, M. Candia Carnevali and F. Bonasoro, Editors. 1998, Balkema: Rotterdam. p. 311-316.

22. Janies, D., **Phylogenetic relationships of extant echinoderm classes**. Canadian Journal of Zoology-Revue Canadienne De Zoologie, 79 (2001): pp. 1232-1250.DOI: DOI 10.1139/cjz-79-7-1232.

23. Telford, M.J., C.J. Lowe, C.B. Cameron, O. Ortega-Martinez, J. Aronowicz, P. Oliveri, and R.R. Copley, **Phylogenomic analysis of echinoderm class relationships supports Asterozoa**. Proc. Biol. Sci., 281 (2014).DOI: Doi 10.1098/Rspb.2014.0479.

24. O'Hara, T.D., A.F. Hugall, B. Thuy, and A. Moussalli, **Phylogenomic Resolution of the Class Ophiuroidea Unlocks a Global Microfossil Record**. Curr. Biol., 24 (2014): pp. 1874-1879.DOI: DOI 10.1016/j.cub.2014.06.060.

25. Reich, A., C. Dunn, K. Akasaka, and G. Wessel, **Phylogenomic Analyses of Echinodermata Support the Sister Groups of Asterozoa and Echinozoa**. Plos One, 10 (2015).DOI: DOI 10.1371/journal.pone.0119627.

26. Cannon, J.T., K.M. Kocot, D.S. Waits, D.A. Weese, B.J. Swalla, S.R. Santos, and K.M. Halanych, **Phylogenomic Resolution of the Hemichordate and Echinoderm Clade**. Curr. Biol., 24 (2014): pp. 2827-2832.DOI: DOI 10.1016/j.cub.2014.10.016.

27. Yun, S.S., M.C. Thorndyke, and M.R. Elphick, **Identification of novel SALMFamide neuropeptides in the starfish *Marthasterias glacialis***. Comp. Biochem. Physiol. A Mol. Integr. Physiol., 147 (2007): pp. 536-42.

28. Conato, C., R. Gavioli, R. Guerrini, H. Kozlowski, P. Mlynarz, C. Pasti, F. Pulidori, and M. Remelli, **Copper complexes of glycyl-histidyl-lysine and two of its synthetic analogues: chemical behaviour and biological activity**. Biochim. Biophys. Acta., 1526 (2001): pp. 199-210.DOI: 10.1016/S0304-4165(01)00127-1.

29. Semmens, D.C., R.E. Dane, M.R. Pancholi, S.E. Slade, J.H. Scrivens, and M.R. Elphick, **Discovery of a novel neurophysin-associated neuropeptide that triggers cardiac stomach contraction and retraction in starfish**. J. Exp. Biol., 216 (2013): pp. 4047-53.DOI: 10.1242/jeb.092171.

30. Haas, B.J., A. Papanicolaou, M. Yassour, M. Grabherr, P.D. Blood, J. Bowden, M.B. Couger, D. Eccles, B. Li, M. Lieber, M.D. MacManes, M. Ott, J. Orvis, N. Pochet, F. Strozzi, N. Weeks, R. Westerman, T. William, C.N. Dewey, R. Henschel, R.D.

Leduc, N. Friedman, and A. Regev, **De novo transcript sequence reconstruction from RNA-seq using the Trinity platform for reference generation and analysis**. Nature Protocols, 8 (2013): pp. 1494-1512.DOI: DOI 10.1038/nprot.2013.084.

31.   Stoll, S. and A. Schweiger, **EasySpin, a comprehensive software package for spectral simulation and analysis in EPR**. J. Magn. Reson., 178 (2006): pp. 42-55.DOI: 10.1016/j.jmr.2005.08.013.

32.   Froncisz, W. and J.S. Hyde, **Broadening by strains of lines in the g-parallel region of Cu2+ EPR spectra.** J. Chem. Phys., 73 (1980): pp. 3123 - 3131.DOI: 10.1063/1.440548.

33.   Marat, K., *SpinWorks 4.1.0*. 2014, University of Manitoba: Canada.

34.   Lever, A.B.P., *Inorganic Electronic Spectroscopy*. 1984, New York: Elsevier.

35.   Stanyon, H.F., X. Cong, Y. Chen, N. Shahidullah, G. Rossetti, J. Dreyer, G. Papamokos, P. Carloni, and J.H. Viles, **Developing predictive rules for coordination geometry from visible circular dichroism of copper(II) and nickel(II) ions in histidine and amide main-chain complexes**. FEBS J., 281 (2014): pp. 3945-54.DOI: 10.1111/febs.12934.

36.   Hureau, C., H. Eury, R. Guillot, C. Bijani, S. Sayen, P.L. Solari, E. Guillon, P. Faller, and P. Dorlet, **X-ray and solution structures of Cu(II) GHK and Cu(II) DAHK complexes: influence on their redox properties**. Chemistry, 17 (2011): pp. 10151-60.DOI: 10.1002/chem.201100751.

37.   Trapaidze, A., C. Hureau, W. Bal, M. Winterhalter, and P. Faller, **Thermodynamic study of Cu2+ binding to the DAHK and GHK peptides by isothermal titration calorimetry (ITC) with the weaker competitor glycine**. J. Biol. Inorg. Chem., 17 (2012): pp. 37-47.DOI: 10.1007/s00775-011-0824-5.

38.   Peisach, J. and W.E. Blumberg, **Structural implications derived from the analysis of electron paramagnetic resonance spectra of natural and artificial copper proteins**. Arch. Biochem. Biophys., 165 (1974): pp. 691-708.DOI: 10.1016/0003-9861(74)90298-7.

39.   Bonomo, R.P., V. Cucinotta, A. Giuffrida, G. Impellizzeri, A. Magri, G. Pappalardo, E. Rizzarelli, A.M. Santoro, G. Tabbi, and L.I. Vagliasindi, **A re-investigation of copper coordination in the octa-repeats region of the prion protein**. Dalton Trans., (2005): pp. 150-8.DOI: 10.1039/b415727c.

40.   Hyde, J.S., B. Bennett, E.D. Walter, G.L. Millhauser, J.W. Sidabras, and W.E. Antholine, **EPR of Cu2+ prion protein constructs at 2 GHz using the g(perpendicular) region to characterize nitrogen ligation**. Biophys. J., 96 (2009): pp. 3354-62.DOI: 10.1016/j.bpj.2009.01.034.

41.   Michael, J.P. and G. Pettenden, **Marine metabolites and metal ion chelation: The facts and the fantasies.** Angew. Chem. Int. Ed. Engl., 32 (1993): pp. 1-23.

42.   Kogut, M.B. and B.M. Voelker, **Strong copper-binding behavior of terrestrial humic substances in seawater**. Environ. Sci. Technol., 35 (2001): pp. 1149-56.DOI: 10.1021/es0014584.

43.   Ndungu, K., **Model predictions of copper speciation in coastal water compared to measurements by analytical voltammetry**. Environ. Sci. Technol., 46 (2012): pp. 7644-52.DOI: 10.1021/es301017x.

44.   Satani, M., K. Takahashi, H. Sakamoto, S. Harada, Y. Kaida, and M. Noguchi, **Expression and characterization of human bifunctional peptidylglycine alpha-amidating monooxygenase**. Protein Expr. Purif., 28 (2003): pp. 293-302.DOI: 10.1016/S1046-5928(02)00684-8.

45. Harrison, M.D., C.E. Jones, M. Solioz, and C.T. Dameron, **Intracellular copper routing: the role of copper chaperones**. Trends Biochem. Sci., 25 (2000): pp. 29-32.DOI: DOI:10.1016/S0968-0004(99)01492-9.
46. Herman, A., H. Kozlowski, M. Czauderna, K. Kochman, K. Kulon, and A. Gajewska, **Gondaoliberin (GnRH) and its copper complex (Cu-GnRH) enzymatic degradation in hypothalmic and pituitary tissue in vitro.** J. Physiol. Pharmacol, 63 (2012): pp. 69-75.
47. Ruppert, E.E., R.S. Fox, and R.D. Barnes, *Invertebrate Zoology: A Functional Evolutionary Approach.* 7th ed. 2003, Belmont, CA: Brooks Cole Thompson.

Figure Legends

Figure 1. C-terminally aligned sequences of SALMFamide neuropeptides derived from L-type SALMFamide precursors in the Asteroidea (*Patiria miniata*, *Asterias rubens* and *Remaster gourdoni*) [1], Ophiuroidea (*Ophionotus victoriae*, *Ophioderma brevispinum* and *Ophiothrix angulata* [2], Echinoidea (*Strongylocentrotus purpuratus*, *Arbacia punctulata* and *Eucidaris tribuloides*) [3] and Holothuroidea (*Apostichopus japonicus*, *Psolus spp* and *Pannychia moseleyi*) [4]. The third amino acid residue from the C-terminal amide has been highlighted in red if it is leucine or isoleucine, yellow if phenylalanine or tyrosine and grey if any other residue. Histidine residues located in the sixth position from C-terminal amide have been highlighted in turquoise.

Figure 2. C-terminally aligned sequences of SALMFamide neuropeptides derived from from F-type SALMFamide precursors in the Asteroidea (*Patiria miniata*, *Asterias rubens* and *Remaster gourdoni*) [1], Ophiuroidea (*Ophionotus victoriae*, *Astrophyton muricatum* and *Ophiothrix angulata* [2], Echinoidea (*Strongylocentrotus purpuratus*, *Arbacia punctulata* and *Lytechinus variegatus*) [3] and Holothuroidea (*Apostichopus japonicus*, *Psolus spp* and *Stichopus chloronatus*) [4]. The third amino acid residue from the C-terminal amide has been highlighted in red if it is leucine or isoleucine, yellow if phenylalanine or tyrosine and grey if any other. Histidine residues located in the sixth position from C-terminal amide have been highlighted in turquoise.

Figure 3. SALMFamide neuropeptides derived from SALMFamide precursors in the Crinoidea (*Antedon mediterranea, Isometra vivipara* and *Oligometra serripinna*). The third amino acid residue from the C-terminal amide has been highlighted in red if it is leucine or isoleucine, yellow if phenylalanine or tyrosine and grey if any other residue. Histidine located in the sixth position from C-terminal amide residues have been highlighted in turquoise.

Figure 4. Copper(II) and nickel(II) titrations monitored by electronic spectroscopy.

(A) Titration of Cu^{2+} (solid black line) into AYHSALPF-NH_2 (100 µM, 10 mM nEM, pH 7.44) results in the formation of a peak at 520 nm. Titration of Ni^{2+} (dashed red line) results in an increase in absorption at 420 nm. (B) Plots of the absorbance at 520 nm (Cu^{2+}) and 420 nm (Ni^{2+}) as a function of added metal. Both curves plateau around 100 µM metal, suggesting 1:1 stoichiometry. (C) Titration of Cu^{2+} (solid black line) and Ni^{2+} (dashed red line) into GYHSGLPF-NH_2 (80 µM, 10 mM nEM, pH 7.44) results in the formation of peaks at 520 nm and 420 nm, respectively. (D) Plots of the absorbance at 520 nm (Cu^{2+}) and 420 nm (Ni^{2+}) as a function of added metal. Both curves plateau around 80 µM metal, suggesting 1:1 stoichiometry. (E) Titration of Cu^{2+} into LHSALPF-NH_2 (110 µM, 10 mM nEM, pH 7.44) generates an absorption band at 600 nm and the binding curve (F) suggests a stoichiometry of 1:1.

Figure 5. Paramagnetic copper causes broadening of GYHSGLPF-NH_2 and LHSALPF-NH_2 ^{1}H NMR spectra. (A) ^{1}H NMR spectra of ~500 µM apo-GYHSGLPF- NH_2 in 10% D_2O/90% H_2O, pH 7.2 (bottom trace) and after the addition of 0.1 equivalent Cu^{2+} (top trace). Assignment of selected perturbed peaks is shown in top trace. (B). ^{1}H NMR spectra of ~500 µM apo-LHSALPF- NH_2 in 10% D_2O/90% H_2O, pH 7.2 (bottom trace) and after the addition of 0.1 equivalent Cu^{2+} (top trace). Assignment of selected perturbed peaks is shown in top trace. Expansion of assigned peaks in both A and B are shown in supplementary material figure S3.

Figure 6. Copper(II) titrations monitored by circular dichroism spectroscopy. (A) CD spectra (300 – 700 nm) were collected as Cu^{2+} was titrated into apo-GYHSGLPF-NH_2 (93 µM, 10 mM nEM, pH 7.7). Peaks at 490 nm and 570 nm are due to d-d transitions and the peak in the near-UV (316 nm) can be attributed to an amide $N^- \rightarrow$ Cu(II) CT. (B) The intensity of the peaks at 316 nm (■) and 490 nm (●) plotted as a function of [Cu(II)]/[GYHSGLPF-NH_2] plateaus at a ratio near one. (C) CD spectra obtained during a titration of apo-LHSALPF-NH_2

(96 μM, 10 mM nEM, pH 7.7) with Cu^{2+} show low intensity peaks at 300 nm (amide N→ Cu(II) CT), 346 nm (imidazole N→ Cu^{2+} CT) and 600 nm (d-d transition). (D) The intensity of the peaks at 300 nm (■) and 346 nm (●) plotted as a function of [Cu(II)]/[LHSALPF-NH$_2$] plateaus at a ratio near one.

Figure 7. X-band EPR spectra of Cu^{II}-bound peptides. (A) First derivative spectrum of [Cu^{II}(GYHSGLPF-NH$_2$)] (ν = 9.433547, 262 μM, 10 mM nEM, pH 7.2, 0.98 equivalents Cu^{2+}), dashed line is simulated spectrum, (B) first derivative spectrum of [Cu^{II}(LHSALPF-NH$_2$)] (ν = 9.433526, 1 mM, 10 mM nEM, pH 7.2, 0.96 equivalents Cu^{2+}), (C) first derivative spectrum of a mixture of [Cu^{II}(LHSALPF-NH$_2$)] (ν = 9.432792, 260 μM, 10 mM nEM, pH 7.2) and apo-GYHSGLPF-NH$_2$ (243 μM, 10 mM nEM, pH 7.2). Inset (c) shows the second derivative spectrum of (C) highlighting the perpendicular region (exp), along with the same region after simulation assuming four (4N) or three (3N) nitrogen donors. (D) Titration of Cu^{2+} into LHSALPF-NH$_2$ (110 μM, 10 mM nEM, pH 7.44) generates an absorption band at 600 nm. Leaving the sample at room temperature for 2 hrs generated a spectrum with broadened d-d transitions.

Figure 8. The occurrence and properties of SALMFamide precursors in species representing each of the five extant echinoderm classes. *A. rub* is the starfish *Asterias rubens* (Asteroidea), *O. vic* is the brittlestar *Ophionotus victoriae* (Ophiuroidea), *S. pur* is the sea urchin *Strongylocentrotus purpuratus* (Echinoidea), *A. jap* is the sea cucumber *Apostichopus japonicus* (Holothuroidea) and *A. med* is the feather star *Antedon mediterranea* (Crinoidea). Signal peptides are shown in blue, spacer peptides are in white, monobasic or dibasic cleavage sites are in green, SALMFamides with a C-terminal FXXamide motif are in yellow, a LXXamide motif are in red and a XXXamide motif are in grey. In addition, SALMFamides containing a histidine residue at the sixth position from the C-terminal amide are marked with H and peptides in which this histidine residue forms an ATCUN motif have been marked

with an asterisk. The data indicate that the common ancestor of all extant echinoderms had a single SALMFamide precursor, including histidine-containing L-type SALMFamides, as in extant crinoids. Then duplication (x2) of the SALMFamide precursor in the common ancestor of extant Eleutherozoa followed by divergence gave rise to two types of precursor: the L-type precursor, which typically includes SALMFamides with a conserved histidine residue, and the F-type precursor. Figure modified from Elphick et al. [17].

Table 1. Spin Hamiltonian parameters for Cu^{II}SALMFamide peptides.

Complex	g_x	g_y	g_z	A_x (^{63}Cu)[a]	A_y (^{63}Cu)[a]	A_z (^{63}Cu)[a]
[Cu^{II}(GYHSGLPF-NH$_2$)]	2.044	2.044	2.176	22.1	22.1	200.9
[Cu^{II}(LHSALPF-NH$_2$)]	2.042	2.042	2.220	-	-	187.5
[Cu^{II}(LHSALPF-NH$_2$) + apoGYHSGLPF-NH$_2$	2.045	2.067	2.207	11.5	12.1	197.3

a. units 10^{-4} cm^{-1}

Figure

Figure 2

P. miniata	**A. rubens**	**R. gourdoni**
PAGSPVFHSALTYa	PAGASAFHSALSYa	Absent
AFHSALPFa	AYHSALPFa	AAYHSGLPFa
GLHSALPFa	AYHTGLPFa	AYHSAMPFa
GFNSALMFa	GFNSALMFa	GYNSALMFa
IHTALPFa	LHSALPFa	MHSALPFa
GYHSALPFa	GYHSALPFa	GYHSGLPFa
GYHTGLPFa	GYHSGLPFa	SFHSGLPFa

1

O. victoriae	**O. brevispinum**	**O. angulata**
SGRRNPSLNSGLIFa	THSLNSGLLFa	SGRSRTYLNSGLLFa
SRLPFHSGLMQa	NKLPFHSGLMQa	SKLPFHSALMQa
SRPQFHTGFMMa	TRPVFHSGFLMa	GKQKAKFHSAMLLa
KAGQRLRFSDGMLFa	KAGARLRWSDGMLFa	KGSRLRWSNGMAFa

2

S. purpuratus	**A. punctulata**	**E. tribuloides**
NMGSIHSHSGIHFa	SRGIYKNSGINFa	SRGIYKNSGINFa
MRLHPGLLFa	MRYHKGISFa	MRYHKGISFa

3

A. japonicus	**Psolus spp**	**P. moseleyi**
VVSRAWSPLVGQTGIAFa	GMRSRWNPLVGQSGLSLa	TARRWSPLVGQTGIAFa
TRSRSMFGNTALPFa	TRSRSSFFGHSALSYa	TRSRAMFGHSALAFa
MGFTGNTGILLa	GGIRGFSGNSATLMa	MGFTGNTGILLa

4

Figure

Figure 3:

Figure

A. mediterranea
ANTSSEPINNWIRALPVLHRGLYFa
NPALSEFMLa
DPSFSSYMLa
NPRLSDLMLa
DPRLSDLMLa
DPRLSDFMLa
DPRLSDFMLa
DPGFSDFTFa
DALGDFMMa
EARLSDYIMa
DPRISDFIMa
KAKFQRPVYPGNa
TPSQIWDTFGAa
FPPAALHKGLYFa

I. vivipara
ANNSAPINNWIRALPLLHQGLYFa
NPALSDFMLa
DPRFSSFMLa
NPRLSDLMLa
DPRLSDLMLa
DPRLSDLMLa
DPGFSDFMLa
DPRLSEFMLa
DPLLSDFMMa
DPRLSDFIMa
DPRLSEFMMa
KVKLHRPSFTGAa
TPSVLWNNLGAa
FPPAALHKGLYFa

O. serripinna
SSNDSAPINNWIRALPLLHQGLFFa
NPAFSDFMLa
DPHLSSFMLa
NPRLSDLMLa
DPRLSDLMLa
DARLSDLMLa
DPRLSDLMLa
DPRFSEFMLa
DPHLSDFMLa
EARLSDFIMa
DPRLSEFMMa
KVKLHRPSFTGAa
TPSVLWNNLGAa
FPPAALHKGLYFa

Figure 3
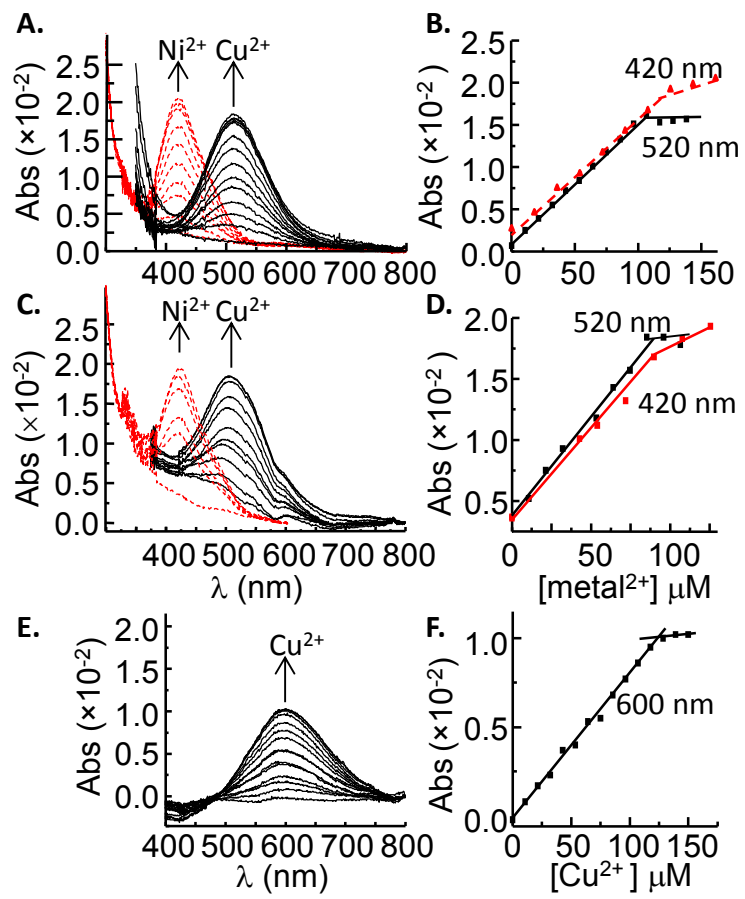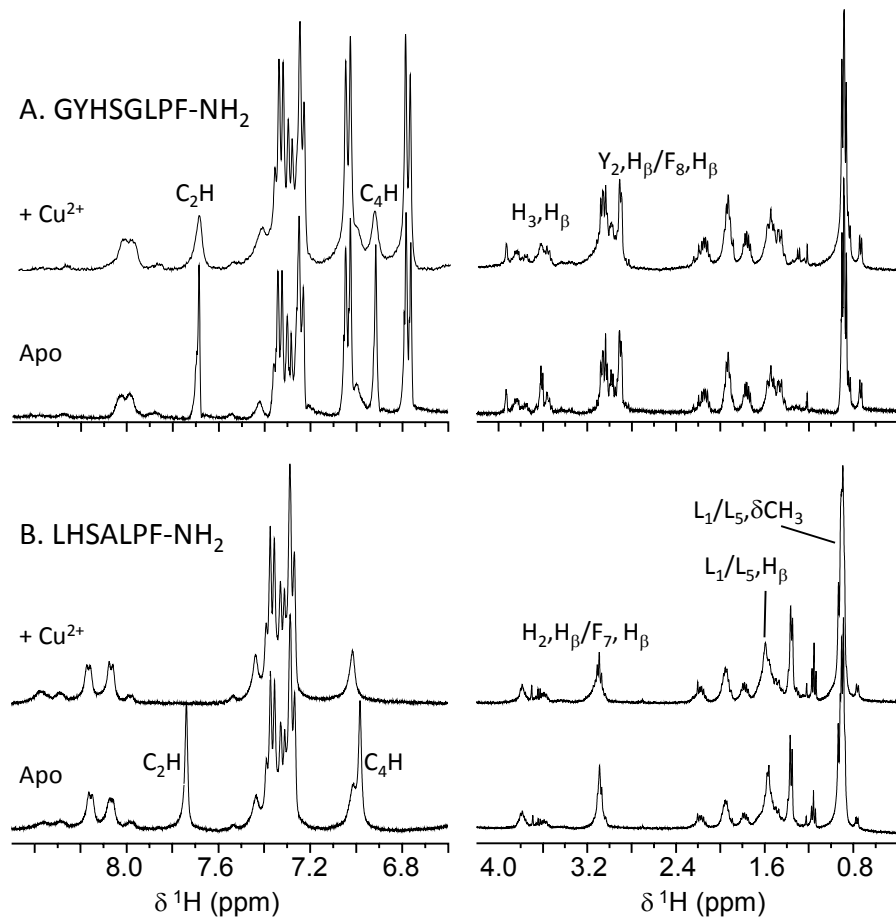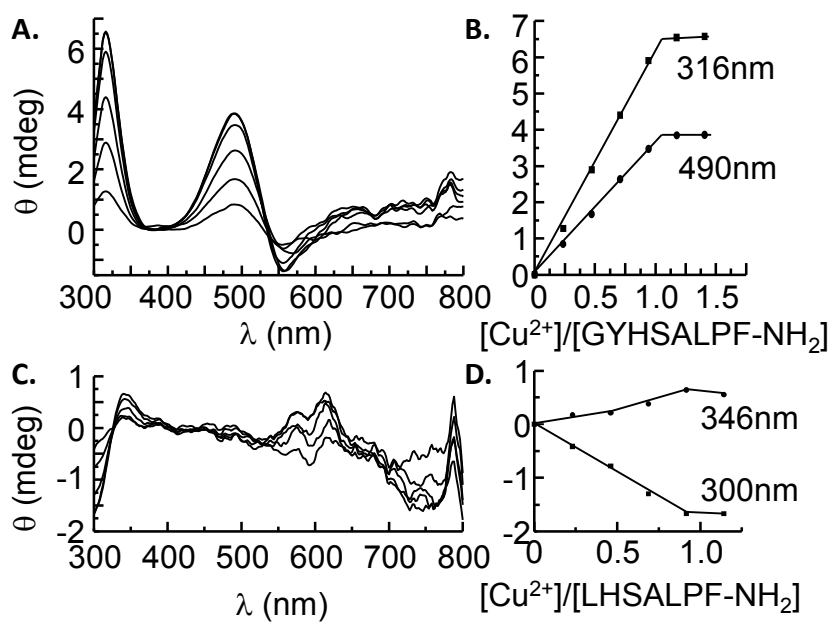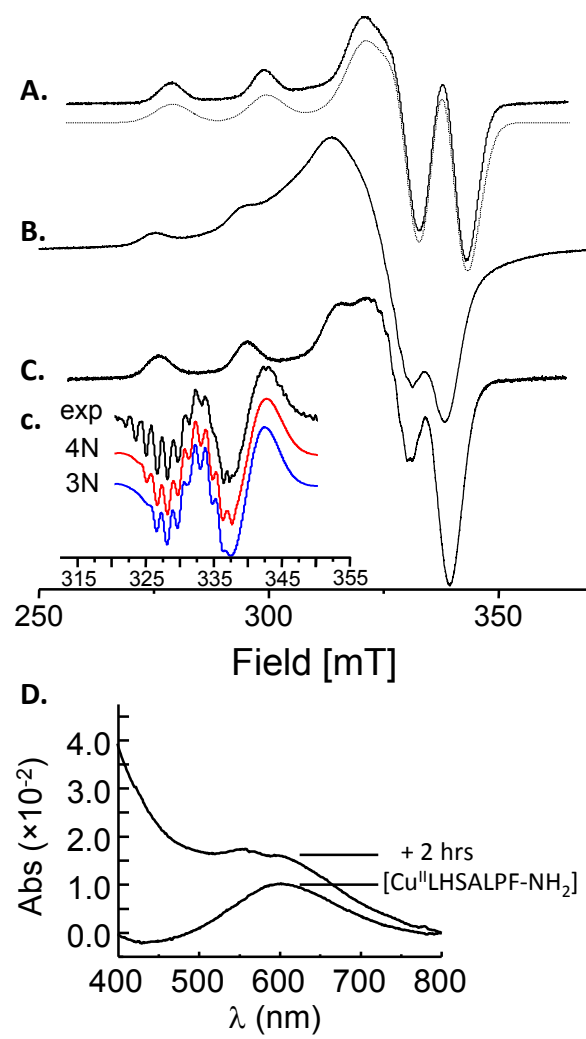
Figure

Figure 4

Figure 5

Figure 6

Figure 7

Supplementary Material

Identification of a neuropeptide precursor protein that gives rise to a "cocktail" of

peptides that bind Cu(II) and generate metal-linked dimers

Christopher E. Jones[a]*, Meet Zandawala[b], Dean C. Semmens[b], Sarah Anderson[b],

Graeme R. Hanson[c]‖, Daniel A. Janies[d] and Maurice R. Elphick[b]*

[a] School of Science and Health, University of Western Sydney, Locked bag 1797,

Penrith, 2751, New South Wales, Australia.

[b] School of Biological & Chemical Sciences, Queen Mary University of London,

Mile End Road, London, E1 4NS, UK.

[c] Centre for Advanced Imaging, The University of Queensland, Brisbane,

Queensland, 4072, Australia

[d] Department of Bioinformatics and Genomics, University of North Carolina at Charlotte,

Charlotte, NC 28223 USA

*To whom correspondence should be addressed:

Christopher E. Jones, School of Science and Health, The University of Western Sydney,

Locked bag 1797, Penrith, NSW, 2759, Australia. Tel: +61 29685 9908; Fax: +61 2 9685

9915; E-mail: c.jones@uws.edu.au

or

Maurice R. Elphick, School of Biological & Chemical Sciences, Queen Mary University of

London, Mile End Road, London, E1 4NS, UK. Tel: 0207 882 6664; Fax: 0207 882 7732; E-

mail: m.r.elphick@qmul.ac.uk

```
1     ctcgagag**tagctacttgacaca**tacacactgcgtaacactcgggtcgcaagctacttct
61    ttgctcgctggccgtagacaactctttgatatctctcgaccaccatcaaaaacgcagaca
121   caacacaatttcgcgtggtttatttaaacgcacacgaggggcctacctgccttgggtttt
181   ttccgggtgtttaattttgtgtactcaccgtcccaaatgaagggccaacaccttctagcc
                                              M  K  G  Q  H  L  L  A    8
241   gtagcagtggttgtcgtcgccggttcgtttggaatcatcgaggcgtactctccatttggg
       V  A  V  V  V  A  G  S  F  G  I  I  E  A  Y  S  P  F  G    28
301   ggctataaccgagcaccttttgacaatgtttgggtgcgagcggacagcatggctcgtgga
       G  Y  N  R  A  P  F  D  N  V  W  V  R  A  D  S  M  A  R  G   48
361   ggctcgacggggggaggacgaagccaacgaacagcgaatgacgggagccaagcgaccggct
       G  S  T  G  E  D  A  N  E  Q  R  M  T  G  A  K  R  P  A   68
421   gg_t_gcctcagcgttccactccgctctgtcgtacggcaaacgaggcgacgatgacagcgcc
       G  A  S  A  F  H  S  A  L  S  Y  G  K  R  G  D  D  D  S  A   88
481   gaagtggagcgccgagcctaccactcggccctgcccttcggcaagagaacacccatcgag
       E  V  E  R  R  A  Y  H  S  A  L  P  F  G  K  R  T  P  I  E  108
541   aaacgcgcctaccacacaggtctccccttcggaaagagggacgacgaagccgccgaacaa
       K  R  A  Y  H  T  G  L  P  F  G  K  R  D  D  E  A  A  E  Q  128
601   gacgccatgatggagaggcgtggcttcaactcggccctgatgttcggtaaacgactacac
       D  A  M  M  E  R  R  G  F  N  S  A  L  M  F  G  K  R  L  H  148
661   agtgctctaccgttcggtaagcgcggctaccacagtgctctgccgttcgggaagagattg
       S  A  L  P  F  G  K  R  G  Y  H  S  A  L  P  F  G  K  R  L  168
721   gataccactgatgaaggagatatcatcgagagaagaggttaccatagcgggctaccgttc
       D  T  T  D  E  G  D  I  I  E  R  R  G  Y  H  S  G  L  P  F  188
781   ggcaagcgcgctactgacgatgaagccgttaatgacatactagaccaattaagaagcgaa
       G  K  R  A  T  D  D  E  A  V  N  D  I  L  D  Q  L  R  S  E  208
841   gagaattgacttttataaagaactgtaatccttaaaaatcagcttatatactaatctaac
       E  N  *                                                    210
901   agtgcttaggatacgacaatatcggttggtgatcagtttagttaccttacaaaac**cctct**
961   **ctcaactagtcatat**caaccttagcgaggacaacgcgggttacacaatgtttcgcatact
1021  taaaaaaa
```

Figure S1: *Asterias rubens* **L-type SALMFamide precursor.** The DNA sequence of a transcript (lowercase, 1028 bases) encoding an L-type SALMFamide precursor protein (uppercase, 210 amino acid residues). The sequence data was first determined by manual assembly of four overlapping contig sequences (1073975, 192719, 104468 and 1057915) and then cDNA sequencing was employed to confirm the section of the DNA sequence bounded by the PCR primer sequences (bold, underline). Bases in the sequenced cDNA that differ from the assembled transcript sequence are shown in underlined italics. The predicted signal peptide of the precursor protein is shown in blue and the seven putative SALMFamide peptides are shown in red, with C-terminal glycine residues that are likely substrates for amidation shown in orange. Putative dibasic cleavage sites (KR, RR) are shown in green and the asterisk shows the position of the stop codon.
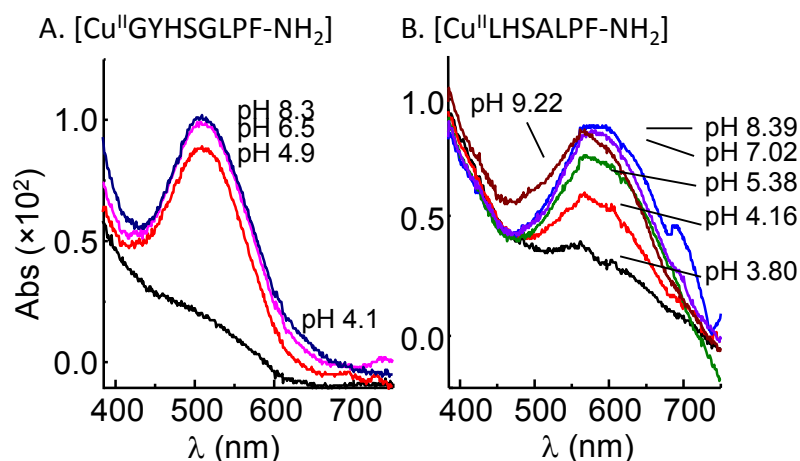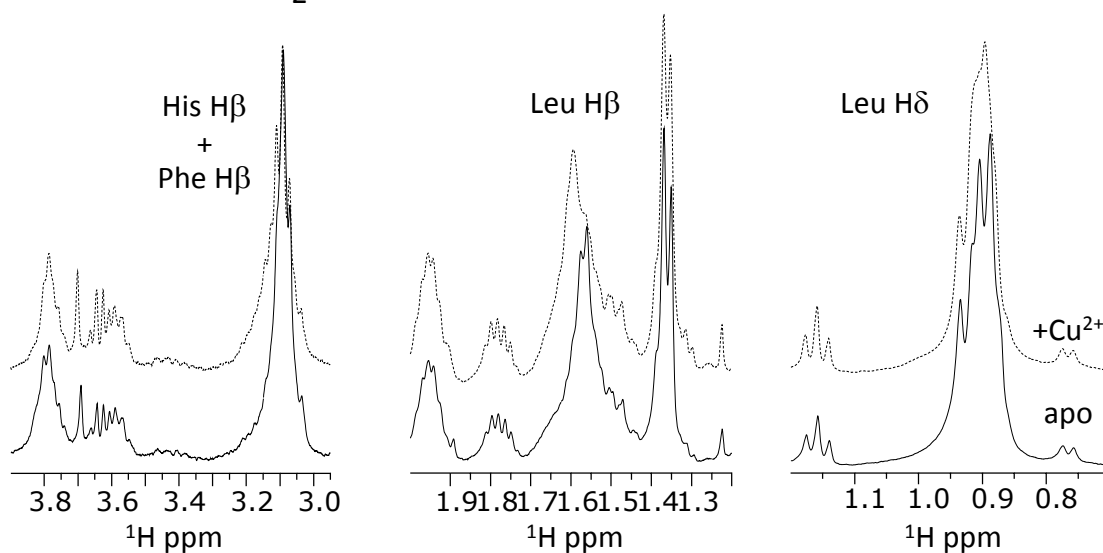
Figure S2. pH titration of [Cu^{II}(GYHSGLPF-NH$_2$)] and [Cu^{II}(LHSALPF-NH$_2$)]. (A). [Cu^{II}GHYSGLPF-NH$_2$] (93.3 μM) was prepared in H$_2$O at an initial pH of 4.1. The pH was increased by the addition of small aliquots of NaOH and the visible electronic spectra obtained at pH values of 4.9, 6.5 and 8.3. (B). [Cu^{II}LHSALPF-NH$_2$] (100 μM) was prepared in H$_2$O at an initial pH of 3.8. The pH was incrementally increased via addition of NaOH and the visible electronic spectra obtained at pH values of 4.16, 5.38, 7.02 and 8.39. Spectra were collected using a Perkin Elmer U-3100 spectrometer and a 10 mm pathlength cuvette.
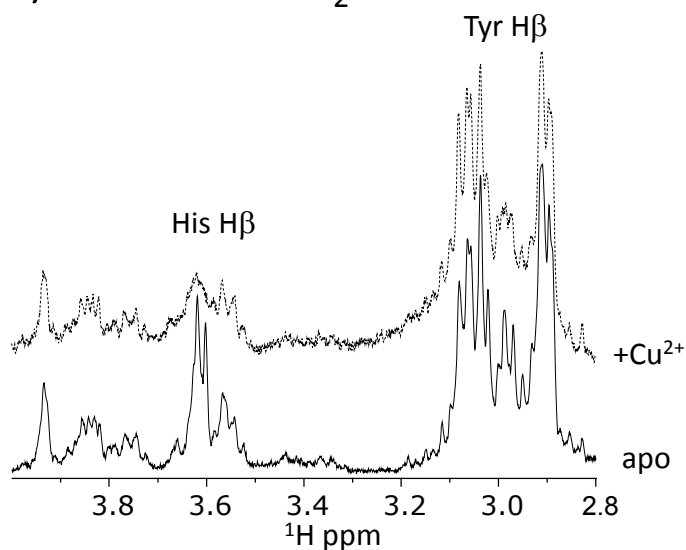
Figure S3. Copper titration of [Cu^{II}(GYHSGLPF-NH$_2$)] and [Cu^{II}(LHSALPF-NH$_2$)].
(A) ^{1}H NMR spectra of ~500 mM apo-GYHSGLPF- NH$_2$ in 10% D$_2$O/90% H$_2$O, pH 7.2
(bottom trace) and after the addition of 0.1 equivalent Cu^{2+} (top trace). Assignment of
selected perturbed peaks is shown in top trace. (B). ^{1}H NMR spectra of ~500 mM apo-
LHSALPF- NH$_2$ in 10% D$_2$O/90% H$_2$O, pH 7.2 (bottom trace) and after the addition of 0.1
equivalent Cu^{2+} (top trace). Assignment of selected perturbed peaks is shown in top trace.

*Conflict of Interest form

Click here to download Conflict of Interest form: Jones_coi_disclosure.pdf

*Conflict of Interest form

Click here to download Conflict of Interest form: Jones_coi_disclosure.pdf